

Electronic and Molecular Structures of Heteroradialenes: A Combined Synthetic, Computational, Spectroscopic, and Structural Study Identifying IR Spectroscopy as a Simple but Powerful Experimental Probe

Carl-Georg Freiherr von Richthofen, Bastian Feldscher, Kai-Alexander Lippert, Anja Stammler, Hartmut Bögge, and Thorsten Glaser

Lehrstuhl für Anorganische Chemie I, Fakultät für Chemie, Universität Bielefeld, Universitätsstr. 25, D-33615 Bielefeld, Germany

Reprint requests to Prof. Dr. Thorsten Glaser. Fax: +49 (0)521 106-6105.

E-mail: thorsten.glaser@uni-bielefeld.de

Z. Naturforsch. 2013, 68b, 64–86 / DOI: 10.5560/ZNB.2013-2241

Received September 10, 2012

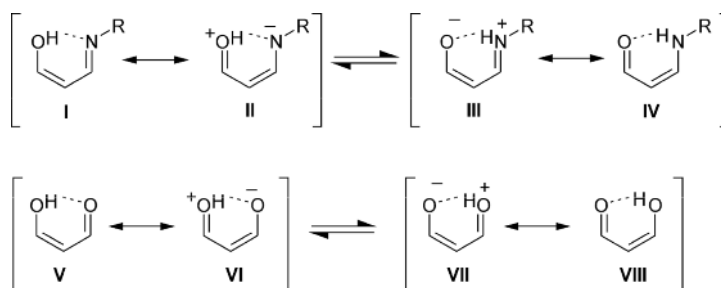
The vicinity of a hydrogen bond donor (O–H) and a hydrogen bond acceptor (C=O or C=N–R) in salicylaldehydes and *ortho*-Schiff bases results in significant structural variations compared to the monosubstituted derivatives that are reflected in the electronic structure and thus in the spectroscopic properties. This interplay between intramolecular hydrogen bonding and multicenter π -electron delocalization is the origin of the concept of resonance-assisted hydrogen bonding (RAHB). Herein, the complexity is extended from one hydrogen bond donor-acceptor pair in salicylaldehyde and *ortho*-Schiff bases to three hydrogen bond donor-acceptor pairs in 2,4,6-tricarbonyl- and 2,4,6-triimine-substituted phloroglucinols (1,3,5-trihydroxybenzene), respectively. To evaluate the changes in the molecular and electronic structures, we have performed a comprehensive computational, spectroscopic, and structural study starting from monosubstituted benzene derivatives as references over *ortho*-disubstituted derivatives to the sixfold-substituted derivatives. Whereas in salicylaldehydes, *ortho*-Schiff bases, and 2,4,6-tricarbonyl-phloroglucinols the phenolic *O*-protonated tautomers represent the energy minima, the *N*-protonated tautomers represent the energy minima in 2,4,6-triimine-phloroglucinols. The analysis provides a keto-enamine resonance structure with six exocyclic double bonds to be dominant for these species reminiscent of [6]radialenes, which were termed heteroradialenes. These heteroradialenes are non-aromatic alicycles. However, the predominance of this resonance structure does not represent a sudden change going from the 2,4,6-tricarbonyl- to the 2,4,6-triimine-phloroglucinols, but a gradual increase of analogous resonance structure contributions is observed even in salicylaldehyde and *ortho*-Schiff bases demonstrating some hetero-*ortho*-quinodimethane character. These changes are, besides in the molecular structures, well reflected in the IR spectra, which can therefore be used as a simple tool to probe the electronic structures in these systems. Interruption of the delocalized π system supporting the intramolecular hydrogen bond, *i. e.* going from 2,4,6-triimine- to 2,4,6-triamine-substituted phloroglucinols, reestablishes an *O*-protonated aromatic phloroglucinol system.

Key words: Density Functional Calculations, IR Spectroscopy, Electronic Structure, Aromaticity

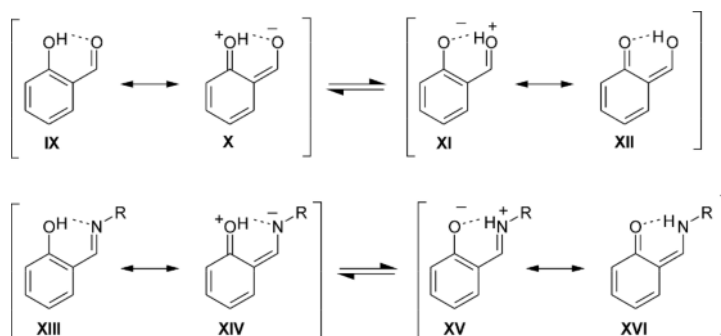
Introduction

The infrared spectra of keto-enamines show characteristic bands in the region of 1700–1400 cm^{-1} the assignments of which lead to many contradictions. Assignments to $\nu(\text{C}=\text{C})$, $\nu(\text{C}=\text{O})$, and $\delta(\text{NH})$ vibrations as well as various combinations have been postulated [1–9]. The difficulty in assigning this region is due to strong coupling of these vibrations, which is

a consequence of π -electron delocalization along the conjugated backbone. This delocalization can be described as a mixture of the resonance forms **III** and **IV** (Scheme 1), where the zwitter-ionic form **III** reduces the double bond character of the C=O bond and increases the double bond character of the C–N bond. The increase of the partial charges of the heteroatoms increases the hydrogen bond acceptor capability of O and the donor capability of N–H lead-



Scheme 1.



Scheme 2.

ing to strong intramolecular hydrogen bonds in these compounds [10]. This strengthening of the hydrogen bond as a consequence of π -electron delocalization is known as resonance-assisted hydrogen bonding (RAHB), a term that has been introduced by Gilli and Gilli in 1989 for malonaldehyde [11, 12]. However, some concerns about the concept of RAHB have been formulated [13–16]. For a recent review see Grabowski *et al.* [17].

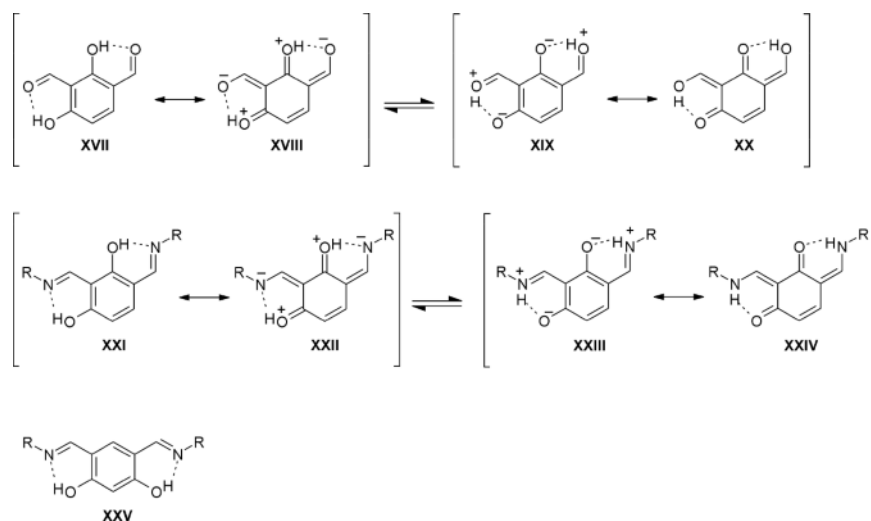
In the symmetric case of malonaldehyde (Scheme 1), the two tautomers **V** and **VIII** as well as **VI** and **VII** are identical. The formal introduction of one amine group leads to an asymmetric donor/acceptor pair, the parent keto-enamines, and thus to an *O*-protonated tautomer (**I** and **II**) and an *N*-protonated tautomer (**III** and **IV**, Scheme 1). While the formally two tautomers of malonaldehyde, **V** and **VIII**, do have the same energy, it is the *N*-protonated tautomer in keto-enamines which is energetically stabilized. This fact is attributed to the stronger proton affinity of amide *versus* alcoholate [10, 18, 19].

Very interesting structures derive from systems where the RAHB unit is fused to aromatic rings. Here, the gain in energy from the RAHB unit competes with the gain in energy from aromatic resonance of

the fused phenyl ring. In salicylaldehyde, tautomer **IX** is more stable than **XII** that is no longer aromatic (Scheme 2) [19, 20]. However, the molecular geometries determined *via* electron diffraction in conjunction with DFT calculations reveal that also in these systems the resonance structure **X** has strong contributions to the overall resonance hybrid so that the hydrogen bond is also resonance-assisted [19, 21, 22]. The same holds true for the salicylaldehyde derivative. Whereas in keto-enamines the *N*-protonated tautomer **IV** represents the minimum, in the aromatic extension the *O*-protonated tautomer **XIII** is more stable due to the stabilizing effect of the aromatic ring, although again with contributions of the resonance structure **XIV** [10, 23].

The influence of the RAHB system on the aromatic ring has been investigated utilizing the harmonic oscillator model of aromaticity (HOMA) [22, 24–26]. The HOMA value is defined as the normalized sum of individual bond lengths R_i and an optimal bond length R_{opt} , which corresponds to full π -electron delocalization.

$$\text{HOMA} = 1 - \frac{\alpha}{n} \sum (R_{\text{opt}} - R_i)^2$$



Scheme 3.

Here n is the number of bonds taken into account and α is an empirical constant ($\alpha = 257.7$) chosen to give a HOMA value of 1 for a system with all bond lengths equal $R_{\text{opt}} = 1.388 \text{ \AA}$ (e. g. benzene) and a value of 0 for a non-aromatic localized 1,3,5-cyclohexatriene. The HOMA value takes the variance of bond lengths as well as the deviation of the mean bond length from R_{opt} into account. Therefore, HOMA values are a suitable tool to evaluate the non-aromatic character of [6]radialene (-2.41) [27] and the fully aromatic character of benzene (0.98). It becomes apparent that even in salicylaldehyde (HOMA = 0.93) the aromaticity is significantly reduced [22].

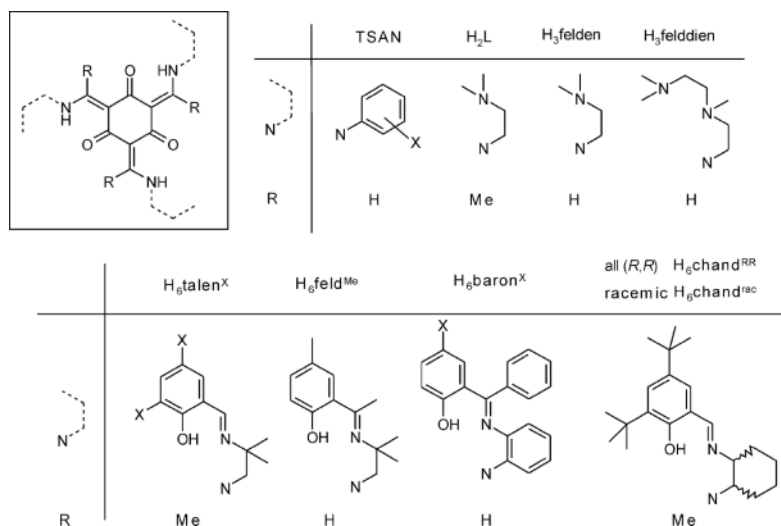
As a further extension, MacLachlan and coworker synthesized salicylaldehydes which are attached to a second RAHB system (Scheme 3), but unfortunately they did not obtain crystals for these compounds [28]. However, structural data of a comparable diketone reveal that also in these compounds contributions of resonance structure **XXVIII** reduce the aromaticity of the ring [29]. They also reacted their systems with aniline derivatives to obtain the analogous imine compounds (Scheme 3). They found the interesting result that if the two RAHB systems are attached in such a way that for both RAHB units the formation of the *N*-protonated tautomer is possible, (**XXI–XXIV**), the gain in energy of the resonance of the aromatic ring is no longer capable to compensate the twofold contribution of the gain in energy of the resonance in the RAHB systems. The consequence is that

the *N*-protonated tautomer becomes the overall minimum with strong contributions of resonance structure **XXIV**. When the simultaneous resonance in both RAHB units is not possible, like for **XXV** (Scheme 3), the *O*-protonated tautomer is the minimum [28]. They extended the system to the trialdehyde and the class of the tris(*N*-salicylideneaniline)s (TSANs, Scheme 4), however without determining the crystal structure of the trialdehyde but with a thoroughly experimental and theoretical analysis of the TSANs.

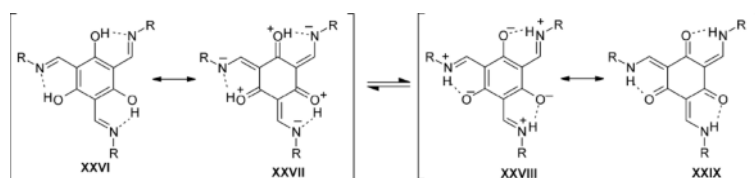
In TSANs [28, 30–44] and our extended phloroglucinol ligands [45–54] (Scheme 4), the *N*-protonated tautomer has been found to be the energy minimum. Moreover, the *N*-protonated tautomer must mainly be considered as the keto-enamine resonance structure **XXIX** with only minor contributions from the phenolate-iminium resonance structure **XXVIII** (Scheme 5). The dominant resonance structure **XXIX** resembles [6]radialenes. Radialenes are cross-conjugated alicyclic hydrocarbons composed of sp^2 -hybridized ring carbon atoms and show as many exocyclic double bonds as possible [55–61]. Therefore **XXIX** was termed a heteroradialene [62].

The scope of this contribution is three-fold:

(1) The symmetrical malonaldehyde and the unsymmetrical keto-enamine have been thoroughly investigated by means of the RAHB concept as well as their aromatic extensions salicylaldehyde and salicylaldimines. In this contribution we extend this discussion to aromatic rings exhibiting three RAHB



Scheme 4.



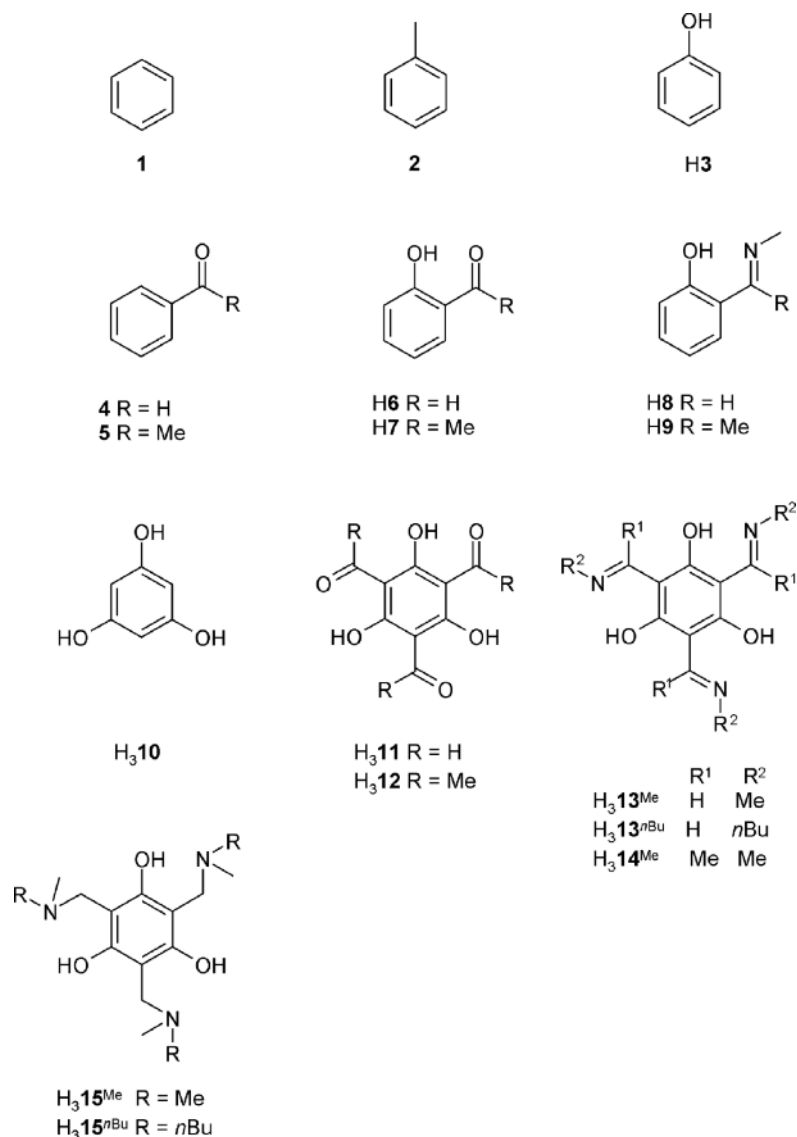
Scheme 5.

units by a comprehensive structural and computational study. We analyse the experimental and calculated molecular structures of phloroglucinol **H₃10** and its 2,4,6-substituted derivatives trialdehyde **H₃11**, triketone **H₃12**, and their imine-derivatives **H₃13^R** and **H₃14^{Me}** (Scheme 6). In order to understand the perturbations induced by individual substituents and their combined influence on an aromatic benzene ring, we start the analysis by the influence of single substituents on benzene (**1–5** in Scheme 6) and the combined influence of two substituents in *ortho*-position (**H₆–H₉**). This forms the basis for the analysis of **H₃10–H₃14^{Me}**.

(2) During our studies on the extended phloroglucinol ligands we observed unusual vibrational features in the FTIR spectra. Especially, prominent features in the 1700–1400 cm⁻¹ region cannot be explained by established assignments and trends derived for imine- and/or salen-type ligands and complexes [46, 47, 49, 51, 63]. However, the realization that the π system of the central phloroglucinol backbone is heavily distorted toward a heteroradialene structure prompted us to ask whether these spectroscopic features may serve

as a convenient method to evaluate the electronic structure of the ligand as well as of the complexes without high-resolution single-crystal diffraction data and NMR spectroscopy, which is not practicable for paramagnetic complexes. We therefore calculated the IR spectra of **1–H₃14^{Me}** that allow us an assignment of the experimental IR spectra and an identification of a unique spectral signature for the heteroradialenes.

(3) We developed the extended phloroglucinol ligand systems in a project to enforce ferromagnetic interactions in *meta*-phenylene-bridged ligand systems by the spin-polarization mechanism [64–79]. These ligands have been applied for the targeted synthesis of single-molecule magnets [80]. However, the exchange coupling mediated by the phloroglucinol bridging unit is weaker as expected, and we attribute this to the loss of the delocalized π system by the heteroradialene formation. In order to strengthen the exchange coupling by restoring the delocalized π system in extended phloroglucinol ligands, we test our hypothesis, that the repression of resonance between the hydrogen bond acceptor and donor would recover the aromatic



Scheme 6.

character of the central benzene ring. Thus, we synthesized, characterized, and calculated the structure and vibrational properties of the amine-derivative **H₃15^R** (R = Me, nBu).

Results

Synthesis and characterization

In order to evaluate the geometry-optimized molecular structures for **H₃11** and **H₃12**, we grew sin-

gle crystals suitable for X-ray diffraction. During our work, the solid-state structure of **H₃12** has been reported [81]. Due to the higher resolution of our measurement, we prefer to use our data for comparison. Fig. 1 shows the molecular structures of **H₃11** and **H₃12**. Whereas the phenolic hydrogen atoms in **H₃12** have been refined, the hydrogen atoms in **H₃11** could be located in a difference Fourier map but not refined. They were therefore included in geometrically generated positions.

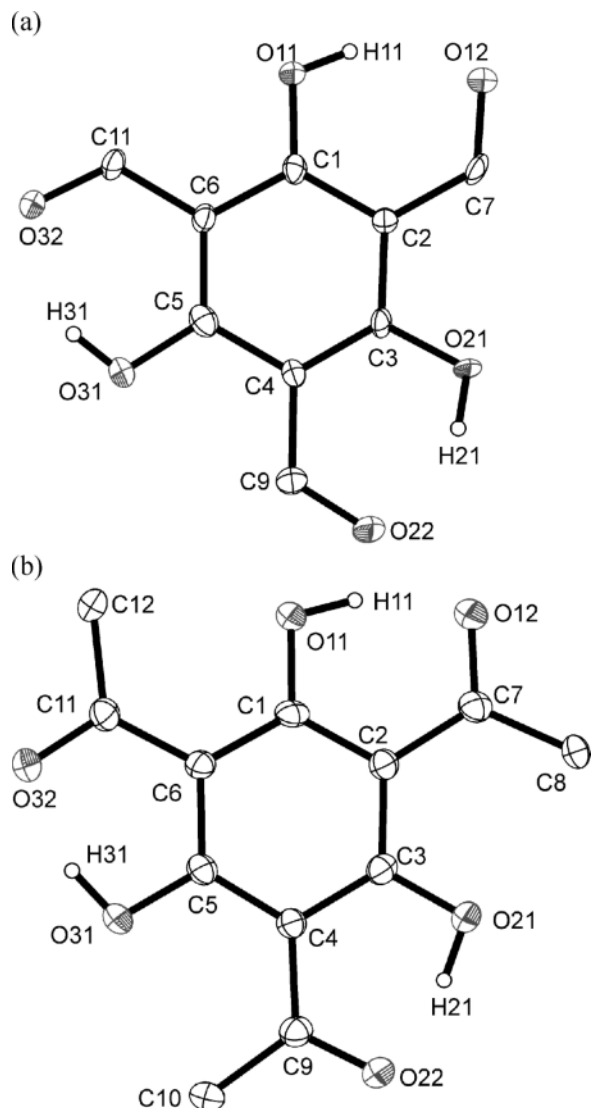


Fig. 1. Molecular structures of a) $H_3\mathbf{11}$ and b) $H_3\mathbf{12}$ obtained by single-crystal X-ray diffraction. Displacement ellipsoids are drawn at the 50% probability level; hydrogen atoms except the phenolic ones are omitted.

In order to evaluate the calculated properties of the trialdimine $H_3\mathbf{13}^{Me}$, the *n*-butyl derivative $H_3\mathbf{13}^{nBu}$ was synthesized analogously to $H_3\mathbf{felden}$ [46] and $H_3\mathbf{felddien}$ [47] by a Schiff base condensation of butylamine and $H_3\mathbf{11}$. The 1H NMR spectrum of $H_3\mathbf{13}^{nBu}$ exhibits four doublets ($J = 14$ Hz) between 8.3–8.0 ppm and two poorly resolved multiplets between 11.5–10.8 ppm (Fig. 2a). This splitting pattern

corresponds to that observed for our *N*-protonated ligands [46, 47, 50, 51]. The presence of four doublets for the vinylic protons is indicative of the presence of two different geometrical isomers (C_{3h} and C_s , Scheme 7) [28, 30, 31, 33–37, 46, 47, 50, 82, 83]. The ratio of the two isomers is *ca.* 1 : 1.7 (C_{3h}/C_s). Addition of D_2O simplifies the 1H NMR spectrum of $H_3\mathbf{13}^{nBu}$ by exchange of the acidic NH hydrogens with deuterium (Fig. 2b). The ^{13}C NMR spectrum of $H_3\mathbf{13}^{nBu}$ exhibits resonances at $\delta = 188.1$ – 182.8 ppm which originate from the *O*-bonded carbon atoms. These chemical shifts are more characteristic for a $C=O$ double bond rather than for a phenolic $C-OH$ single bond [84]. Although a recent report described $H_3\mathbf{13}^{nBu}$ as the *O*-protonated tautomer [85], we propose that the spectroscopic data of $H_3\mathbf{13}^{nBu}$ point to the *N*-protonated tautomer with strong contributions of resonance structure **XXIX** (Scheme 5).

The IR spectrum of $H_3\mathbf{13}^{nBu}$ exhibits prominent bands at 1611, 1547, and 1452 cm^{-1} and the UV/Vis spectrum shows strong absorption maxima at 29 660 and 33 910 cm^{-1} ($\epsilon \approx 24.7$ and $21.0 \times 10^3 M^{-1} cm^{-1}$, respectively). These absorption maxima are also present in the UV/Vis spectra of other of our extended phloroglucinol ligands (Fig. 3) and have been assigned to the heteroradialene backbone [46, 47].

In order to evaluate the changes induced by substitution of the “imine” groups by amine groups, the saturated trisamine $H_3\mathbf{15}^{nBu}$ was synthesized by a Mannich reaction adapted from a literature procedure from phloroglucinol, methyl butylamine, and formaldehyde [86]. The 1H NMR spectrum exhibits singlets at $\delta = 9.03$ and 3.70 ppm for the phenolic *OH* and the benzylic CH_2 methylene protons, respectively. The ^{13}C resonance at 156.2 ppm for the phenolic carbon atom is in agreement with that of $H_3\mathbf{10}$ (158.9 ppm). The IR spectrum exhibits strong bands at 1632, 1456, and 1111 cm^{-1} , and the UV/Vis spectrum exhibits only a weak band at 35 800 cm^{-1} , contrary to $H_3\mathbf{13}^{nBu}$ (Fig. 3).

Geometry-optimized structures

We have used DFT with the BP86 functional and a TZVP basis set as a reliable, non-expensive method to optimize the molecular structures of **1**– $H_3\mathbf{15}^{Me}$ (Scheme 6) and to calculate their IR vibrational frequencies. The results of the DFT calculations are first calibrated and evaluated with reference to ex-

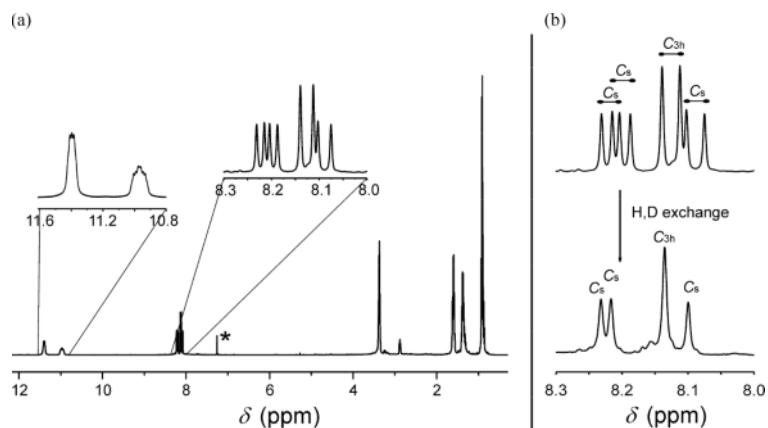
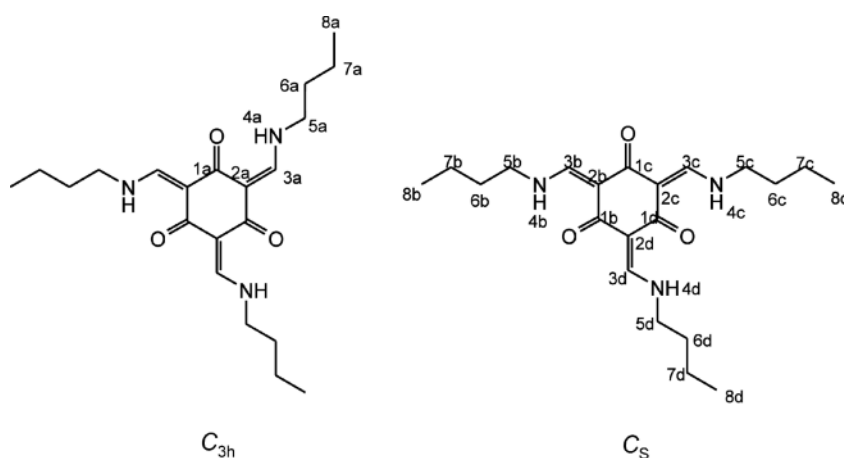


Fig. 2. a) ^1H NMR spectrum of $\text{H}_3\mathbf{13}^{n\text{Bu}}$ in CDCl_3 measured at 500 MHz (* = CHCl_3); b) simplification of the ^1H NMR spectrum *via* deuteration of NH by addition of deuterium oxide in CDCl_3 measured at 300 MHz.



Scheme 7.

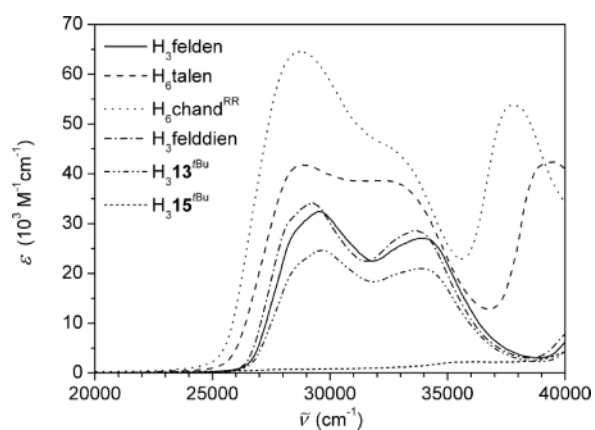


Fig. 3. Electronic absorption spectra of H_3felden , H_6talen , $\text{H}_6\text{chand}^{\text{RR}}$, $\text{H}_3\text{felddien}$, $\text{H}_3\mathbf{13}^{n\text{Bu}}$, and $\text{H}_3\mathbf{15}^{n\text{Bu}}$.

perimental structural and infrared spectroscopic data. We included mono- and di-substituted benzene derivatives ($\mathbf{1}$ – $\mathbf{H9}$) and phloroglucinol $\text{H}_3\mathbf{10}$ as references for our discussion on the hexasubstituted benzene derivatives ($\text{H}_3\mathbf{11}$ – $\text{H}_3\mathbf{15}^{\text{Me}}$). Although many quantum-chemical reports on $\mathbf{1}$ – $\mathbf{H310}$ have appeared in the literature [87–100], an appropriate comparison requires calculations by the same computational method.

Fig. 4 compares calculated bond lengths for the individual molecules to experimental data (single-crystal X-ray diffraction and/or – if available – gas-phase electron diffraction) by three digits. In the following discussion, we mostly compare bond lengths by two digits in order 1) to avoid an overinterpretation of theoretical and experimental accuracy and 2) to avoid the impression of differences that are chemically not significant.

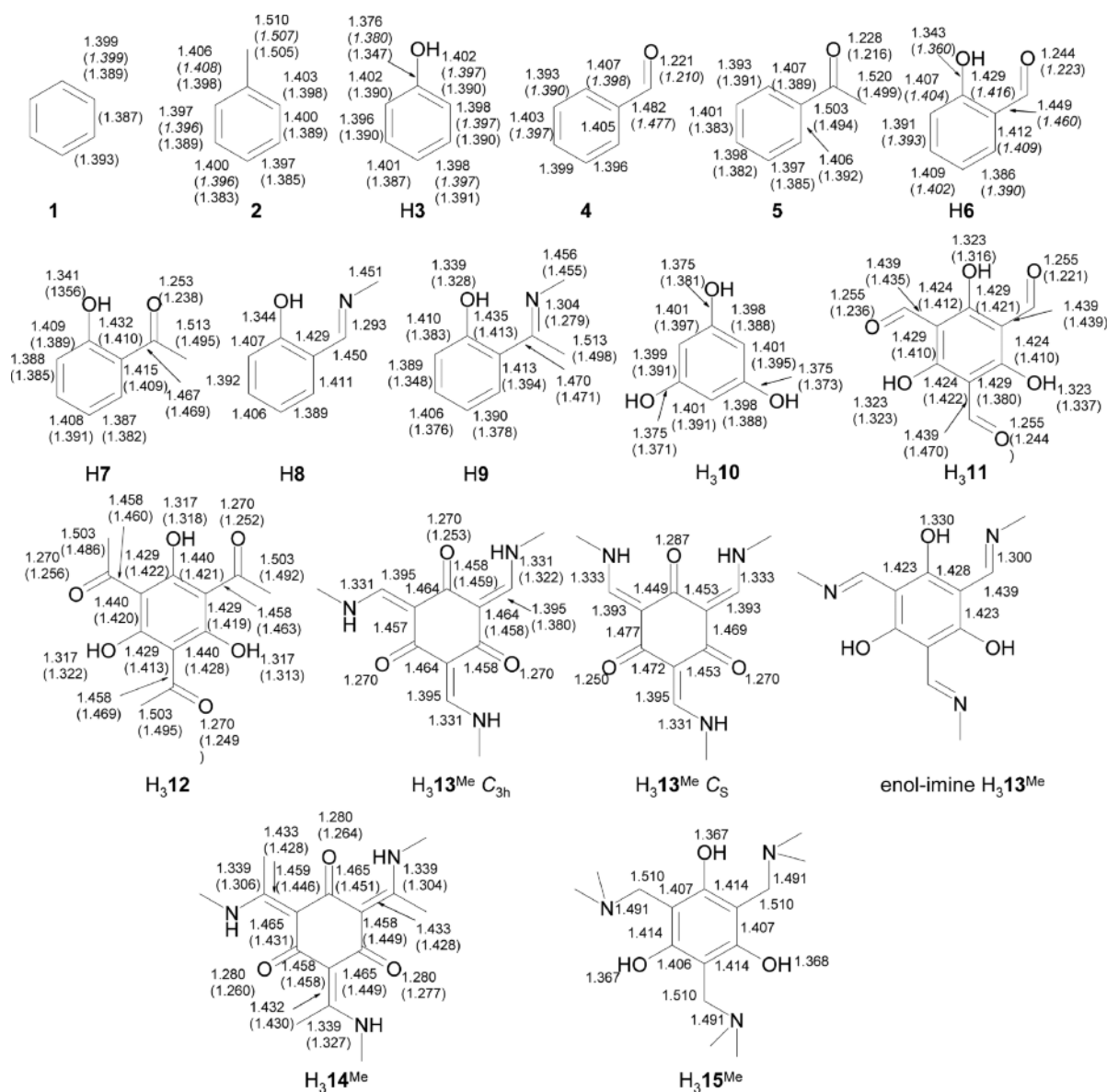


Fig. 4. Comparison of calculated bond lengths with experimental values. Experimental data from single-crystal X-ray diffraction (CRD) are given in normal script in parentheses, and gas-phase electron diffraction (GED) data are given in italics in parentheses. Experimental data are obtained from the following references: **1** GED [101], XRD [102]; **2** GED [103, 104], XRD [105]; **H₃** GED [106], XRD [107]; **4** GED [21]; **5** XRD [108]; **H₆** GED [21]; **H₇** XRD [109]; **H₉** XRD [110]; **H₃10** XRD [111]; **H₃11** this work; **H₃12** this work; **H₃13^{Me}** XRD H₆baron^{Me} [51]; **H₃14^{Me}** H₆chand^{rac} has been used as reference [53].

The experimental molecular structures of **1** to **H₃10** are well reproduced by the calculations. The geometry-optimized bond distances fit the experimentally determined data, so that most values coincide in the

second digit with only very few exceptions that exceed a ± 0.02 Å range like in **H₇**. However, even in such cases the chemical trends are well reproduced. The strongest difference is found for the C–O bond

length in phenol (**H3**) (1.35 Å in solid state; 1.38 Å calculated). However, the gas-phase C–O bond length of 1.38 Å matches the calculated value revealing the known problem of comparing calculated gas-phase structures to experimental solid-state structures. In the following, the geometry-optimized and experimentally derived molecular structures of the hexasubstituted benzene derivatives are compared in some more detail.

The geometry optimization of the trialdehyde **H311** and the triketone **H312** results in C_{3h} symmetric planar molecules with carbonyl and hydroxyl groups in the molecular plane with very short O···O distances of 2.49 and 2.40 Å in **H311** and **H312**, respectively. The shorter distance in **H312** is accompanied by a smaller $C^{ar}-C^{C=O}-O$ angle of 119.4° compared to 122.5° in **H311**. The shorter O···O distance also leads to a longer O–H distance of 1.09 Å in **H312** compared to 1.05 Å in **H311**. The results on **H312** nicely reproduce results of a former study [112].

These calculated structures are confirmed by the experimentally determined structures (Fig. 1). Both molecules are almost planar C_{3h} symmetric with some minor deviations from ideality evidenced for example in the bond lengths distribution (Fig. 4). The difference in the O···O distances is also experimentally evident (2.59 Å in **H311** vs. 2.42 Å in **H312**).

For the trialdimine derivative **H313^{Me}**, we could locate three minima in the potential energy surface: an *O*-protonated enol-imine of C_{3h} symmetry, an *N*-protonated heteroradialene of C_{3h} symmetry, and an *N*-protonated heteroradialene of C_s symmetry. The C_{3h} heteroradialene represents the global minimum with the C_s heteroradialene ~ 1.7 kcal mol⁻¹ and the enol-imine ~ 9.2 kcal mol⁻¹ higher in energy. All three minima exhibit planar structures with the imine or enamine groups in the plane of the central backbone. The O···N and O–H distances for the enol-imine form are 2.50 and 1.08 Å, respectively, while the values for the C_{3h} heteroradialene form are 2.61 Å for the O···N and 1.04 Å for the N–H distances. In the C_s symmetric form, one enamine group is rotated by 180° along the $C^{ar}-C^{CN}$ vector (Scheme 7). This results in different hydrogen bonding scenarios for the three oxygen atoms: one with two N–H···O hydrogen bonds (N···O distances 2.63, N–H distances 1.04 Å), one with one N–H···O hydrogen bond (N···O distance 2.62, N–H distance 1.04 Å), and one without hydrogen bonding. The bond lengths differ tremendously between these three isomers (Fig. 4).

The central backbone of **H6baron^{Me}** corresponds directly to that of **H313^{Me}**. The molecular structure of **H6baron^{Me}** was established by single-crystal X-ray diffraction to be in the *N*-protonated C_{3h} heteroradialene form corroborated by NMR spectroscopy in solution [51]. It is rewarding to see that the experimentally determined molecular structure of **H6baron^{Me}** best reproduces the calculated global minimum with C_{3h} symmetric *N*-protonated heteroradialene with regard to symmetry, protonation, and bond lengths (mean O···N distances of 2.59 Å in **H6baron^{Me}**) (Fig. 4).

The geometry optimization of the triketimine **H314^{Me}** provided only the C_{3h} symmetric, *N*-protonated heteroradialene form irrespective of the starting geometry. The N–H and O···N distances are 1.06 and 2.49 Å, respectively. The shorter O···N distance in **H314^{Me}** than in **H313^{Me}** (2.61 Å) results in a smaller $C-C^{C=N}-N$ angle of 118.7° in **H314^{Me}** than in **H313^{Me}** (124.7°). Moreover, in contrast to the C_{3h} symmetric heteroradialene **H313^{Me}**, the six substituents in the heteroradialene **H314^{Me}** push themselves out of the central plane resulting in O=C–C=C dihedral angles of $\sim 6^\circ$.

This calculated model nicely reproduces the experimental structure by the central backbone of **H6chand^{rac}**, although **H6chand^{rac}** exhibits stronger deviations from C_3 symmetry. Nevertheless, the mean O···N distances of 2.50 Å compares well to that of **H314^{Me}** [53]. The strongest difference is in the $C(sp^2)-N$ bond (mean value 1.31 Å in **H6chand^{rac}** vs. 1.34 Å in **H314^{Me}**), which may be related to a cyclohexyl vs. a methyl substituent at the nitrogen atom.

The DFT-optimized structure of the triamine **H315^{Me}** exhibits almost C_3 symmetry with the amine groups rotated out of the central plane. The proton is bonded to the phenolic oxygen atom with a distance of 1.02 Å and forms a hydrogen bond with the amines at O···N distances of 2.66 Å. Unfortunately, we are not aware of a structural report for a molecule that resembles the central backbone of **H315^{Me}**.

IR spectra: comparison of calculated to experimental results and assignments

There have been numerous calculations of IR spectra of benzene and its substituted derivatives by DFT and MO methods dealing with a) the quantitative reproduction of the spectra as a function of the computational method used, on the basis sets, and – in

the case of DFT – the functional used, and b) with the assignment of the observed vibrations [87–93, 95–100, 113]. Therefore, we do not discuss the results in detail, but rather evaluate the computational method and emphasize some specific results of these reference molecules that are valuable for the later discussion.

It must be emphasized that a) overtones and combination bands cannot be reproduced by the chosen DFT methodology and that b) the calculated spectra are for the gas phase whereas experimental spectra were measured for solid compounds in KBr disks and for liquid compounds as films on KBr disks. Therefore, there must be significant differences between experimental and calculated spectra. *E. g.*, the C–H stretch of the formyl group of benzaldehyde **4**, calculated with one band at 2781 cm^{-1} , exhibits four bands in this region with two intensive bands at 2820 and 2737 cm^{-1} . As this stretching mode is not degenerate, this splitting demonstrates the difference between gas-phase calculation compared to an experimental film spectrum. Considering these limitations, the comparison of experimental and calculated IR spectra of **1–H9** shows a good reproduction of the experimental spectra by the calculations. Interestingly, the experimental spectra are better reproduced the less symmetric the molecule is.

The calculated O–H stretch of phenol **H3** at 3685 cm^{-1} corresponds to the gas-phase molecule without intermolecular hydrogen bonds and can therefore not match the experimentally observed broad band at around 3350 cm^{-1} in the solid state. This applies to the O–H stretching modes of all other molecules as well. Furthermore, the calculated IR spectrum of phenol **H3** exhibits a very intense vibration at 1161 cm^{-1} without matching an experimental band. This vibration has also been obtained by other DFT calculations [93, 95, 96, 98, 113]. Despite of some C–C stretch character, this vibration has C–H and O–H in-plane bending character and has been assigned to a strong band at 1177 cm^{-1} in the IR spectrum of phenol vapor [114, 115].

A special emphasis is placed on the spectra in the $1700\text{--}1300\text{ cm}^{-1}$ region as extended phloroglucinol ligands and complexes exhibit characteristic bands in this region [45–54, 63, 116–125]. This region is dominated in benzene derivatives by C–C ring stretching modes. As there are six C–C bonds, there must be six ring stretches. However, the restrictions of normal modes naturally results in mixing with other vibra-

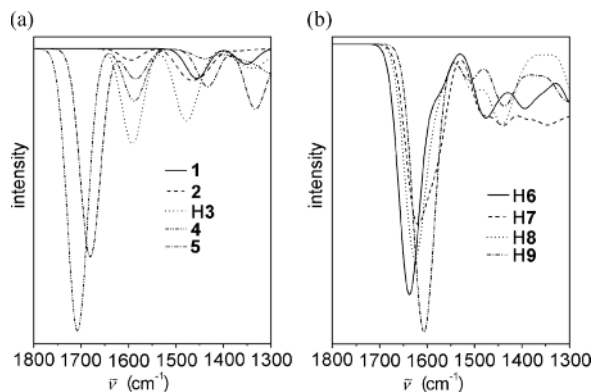


Fig. 5. Comparison of calculated IR spectra emphasizing C=O and C=C stretching modes: a) **1–H5** and b) **H6–H9**.

tions. This prohibits in most cases simple assignments to specific parts of the molecules.

For **1–5**, six normal modes with predominant C–C stretch character are calculated between $1600\text{--}1330\text{ cm}^{-1}$. The lower the energy, the more C–H in-plane bending modes are mixed in. However, the most important point is that the intensities of these six vibrations differ significantly upon variation of the substituents (Fig. 5a). For benzene **1**, two vibrations at 1453 and 1351 cm^{-1} possess significant IR intensities, while the vibrations at 1592 , 1588 , 1469 , and 1331 cm^{-1} do not. For example, the vibration at 1592 cm^{-1} in benzene **1** does not result in a change of the dipole moment. Introduction of one substituent reduces the symmetry so that the dipole moment of the C–C stretch of toluene **2** at 1596 cm^{-1} , that corresponds to the 1592 cm^{-1} vibration in **1**, varies during the vibration and thus gains IR intensity. The more polar the substituent, the stronger the intensity of this stretch (relative intensities for X = -H, -CH₃, -COCH₃, -CHO, -OH: 0, 9, 20, 36, 39). Overall, toluene **2** exhibits three C–C stretches with significant IR intensities (1596 , 1485 , 1460 cm^{-1}), while phenol **3** shows five such C–C stretches (1597 , 1587 , 1483 , 1459 , 1360 cm^{-1}). Therefore, variations in the observed IR spectra do not necessarily reflect variations in the electronic structure.

Our calculations of the IR spectra of **H6–H9** reproduce calculated IR spectra that have already been reported in the literature [96–99]. Compounds **4** to **H9** possess a C=O or a C=N double bond and their IR spectra exhibit besides the C=C ring stretches an intense band in the $1710\text{--}1620\text{ cm}^{-1}$ region usually as-

signed to the stretching frequency of a C=O or C=N double bond. The intense vibrations at 1708 cm^{-1} for **4** and at 1681 cm^{-1} for **5** (Fig. 5a) clearly have the C=O stretch as main contribution. The slight shift to lower energy of this band from **4** to **5** can also be seen in the experimental IR spectra (1703 cm^{-1} for **4** and 1684 cm^{-1} for **5**).

However, the strong band at 1637 cm^{-1} in **H6** (Fig. 5b) is a superposition of two vibrations: the higher energy vibration at 1638 cm^{-1} contains significant contributions from C=C ring stretching and $\delta(\text{C}-\text{O}-\text{H})$ deformation modes, despite the C=O stretching mode character. The second lower energy vibration at 1607 cm^{-1} contains besides significant C=C also some C=O stretching character. The same holds true for **H7**, which has two vibrations at 1625 and 1594 cm^{-1} (Fig. 5b) both with C=O and C=C stretch character, while the 1576 cm^{-1} mode mainly contains C=C stretching vibrations. **H8** contains two vibrations at 1630 and 1622 cm^{-1} (Fig. 5b) both of mixed C=N and C=C stretch character, while the band at 1579 cm^{-1} mainly involves C=C stretch character. Contrary to **4**–**H8**, the high-energy vibration in **H9** at 1613 cm^{-1} mainly has C=C ring stretching character with almost no C=N stretching character! The two following vibrations at 1604 and 1586 cm^{-1} are mixed C=N and C=C stretching modes.

The calculated C–O stretch in **H3** at 1244 cm^{-1} shifts to 1292 cm^{-1} in **H6**. In **H7**, this mode at 1305 cm^{-1} already contains severe mixing with the $\text{C}^{\text{C}=\text{O}}-\text{C}^{\text{CH}_3}$ stretching mode. This tendency is again strengthened in **H8**–**H9**. In aldimine **H8**, the C–O stretching mode appears at 1285 cm^{-1} , while in ketimine **H9** two modes at 1311 and 1269 cm^{-1} contain C–O stretching character, mixed with the $\text{C}^{\text{C}=\text{N}}-\text{C}^{\text{CH}_3}$ stretching mode.

The comparison of the experimental and calculated IR spectra of **H3****10**–**H3****12** shows a good reproduction of the experimental spectra by the calculations. Two main C=C stretches at 1613 and 1609 cm^{-1} (Fig. 6a) are calculated for phloroglucinol **H3****10** [100] that are of higher intensity than in phenol **H3**. The three local C–O stretches couple to provide three normal modes: the symmetric one at 1346 cm^{-1} with almost no IR intensity and two asymmetric ones at 1131 and 1129 cm^{-1} . This coupling prohibits a simple comparison to the C–O stretch of phenol **H3** at 1244 cm^{-1} . These results allow an assignment of the experimentally observed IR vibrations in **H3****10**: 1625 cm^{-1} mainly C=C stretching modes, 1540 – 1500 cm^{-1} C=C ring stretching modes mixed with C–H bending modes, 1157 cm^{-1} C–O stretching mode.

The calculations for trialdehyde **H3****11** provide two intense vibrations at 1640 cm^{-1} that mainly consist of C=C stretching and C–O–H deformation modes. The symmetric C=O stretch at 1628 cm^{-1} contains almost no IR intensity. Two intense asymmetric C=O modes coupled with C=C stretching modes appear at 1590 and 1588 cm^{-1} (at lower energies than for **H6** 1639 cm^{-1}). Two C=C stretching modes coupled with C–O–H bending modes appear at 1308 cm^{-1} with significant IR intensity. It is difficult to identify a vibration of a symmetric C–O stretching mode, since the vibrations at 1202 and 1200 cm^{-1} possess strong C–O stretching mixed with C=C and C–C stretching character. This allows the assignment of the experimentally observed IR vibrations of trialdehyde **H3****11**: 1642 cm^{-1} mainly C=C stretch, 1606 cm^{-1} mainly C=O stretch, 1435 cm^{-1} C=C stretch mixed with C–O–H bending, 1253 cm^{-1} mixed C=C and C–C stretching modes, 1194 cm^{-1} C–O stretch mixed with C=C and C–C stretches.

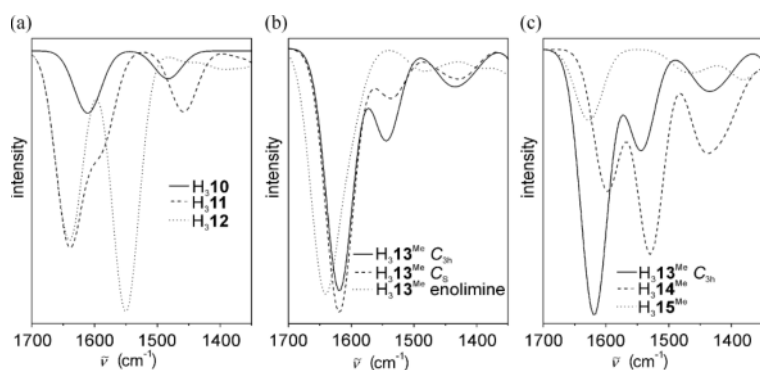


Fig. 6. Comparison of calculated IR spectra emphasizing C=O and C=C stretching modes: a) **H3****10**–**H3****12**, b) the three isomers of **H3****13**^{Me}, and c) **H3****13**^{Me}–**H3****15**^{Me}.

Three O–H stretching modes are calculated for triketone **H₃12** at 2035, 2032, and 2027 cm⁻¹. This allows assigning the unusual vibrations in the experimental IR spectrum of **H₃12** in the range of 1900 to 2700 cm⁻¹ to the O–H stretching modes. The calculated vibrations from 1640 to 1100 cm⁻¹ exhibit strong mixing of several vibrational modes, prohibiting a simple assignment. Two intense bands at 1642 and 1639 cm⁻¹ are composed of C=O, C=C stretching and C–O–H bending modes. A low intensity band at 1628 cm⁻¹ is a symmetric C=O stretching mode. Two strong bands at 1551 and 1550 cm⁻¹ are mixed C=C and C=O stretching modes. Two medium to weak bands at 1277 and 1275 cm⁻¹ are mainly C–C stretching modes and two weak bands at 1196 cm⁻¹ may be attributed to a mixed C–O and C=C stretching mode. This strong mixing of modes makes an assignment of the experimentally observed vibrations less straightforward. However, the two strong bands at 1626 and 1582 cm⁻¹ are mixed C=O and C=C stretching modes. An assignment to a C–O mode is not feasible.

The calculated IR spectrum of the C_{3h} symmetric *N*-tautomer of **H₃13^{Me}** exhibits three C=C stretching modes of the exocyclic double bonds in the range 1600 to 1700 cm⁻¹ with the symmetric combination at 1663 cm⁻¹ with no IR intensity and two strong asymmetric modes at 1621 and 1617 cm⁻¹ (Fig. 6b). In the range 1500 to 1600 cm⁻¹ only three modes of medium intensity at 1545, 1544 and 1542 cm⁻¹ appear, which correspond to asymmetrical C=O stretch. Below 1500 cm⁻¹ several mainly very weak bands with coupled vibrations appear with two vibrations of significant intensity at 1444 and 1442 cm⁻¹ of C=C stretching modes coupled with differing stretching modes and vibrations over the whole molecule.

The calculated IR spectrum of the C_s isomer of **H₃13^{Me}** looks similar to that of the C_{3h} symmetric form. The exocyclic C=C stretching mode around 1620 cm⁻¹ is almost identical to that of the C_{3h} symmetric form, while the C=O stretching modes in the range 1528 to 1568 cm⁻¹ exhibit only half the intensity of that of the more symmetric isomer. In analogy to the calculated structure, the C_s symmetric *N*-protonated tautomer **H₃13^{Me}** contains three different C=O vibrations: at 1568 cm⁻¹ for the C=O group without hydrogen bonding, at 1543 cm⁻¹ for the C=O group with one N–H hydrogen bond, and at 1528 cm⁻¹ (Fig. 6b).

The calculated IR spectrum of the C_{3h} symmetric enol-imine tautomer of **H₃13^{Me}** exhibits significant

differences and is dominated by two very strong vibrations: an O–H stretching mode at 2041 cm⁻¹ and a vibration at 1643 cm⁻¹ with mainly C=C ring stretching character mixed with C–O–H deformation modes. Two C=N imine stretching modes of medium intensity appear at 1608 and 1601 cm⁻¹. Most importantly, there is no counterpart in the 1540 to 1550 cm⁻¹ region corresponding to the C=O vibrations in the *N*-protonated forms (Fig. 6b).

In this respect, the experimental spectrum of **H₃13^{nBu}** is best reproduced by the C_{3h} symmetric heteroradialene form. It must be emphasized that the synthesized compound **H₃13^{nBu}** comprises three *n*-butyl substituents at the nitrogen atoms in contrast to the methyl substituents of the truncated molecule **H₃13^{Me}** for the DFT calculations. This leads to many C–H deformation modes around 1500 cm⁻¹, which explains the higher intensity of the experimental spectrum of **H₃13^{nBu}** in this area in comparison to that for calculated **H₃13^{Me}**. However, these calculated data allow the assignment of the experimental band at 1611 cm⁻¹ to be dominated by C=C stretches of the exocyclic double bonds, the band at 1547 cm⁻¹ to be mainly composed of C=O stretching modes and the band at 1452 cm⁻¹ to feature ring stretching modes coupled with C=C vibrations of the exocyclic double bonds.

The calculated IR spectrum of **H₃14^{Me}** (Fig. 6c) exhibits three stretching modes of the exocyclic double bonds (symmetric at 1611 cm⁻¹ with almost no IR intensity, and at 1601 and 1595 cm⁻¹ asymmetric with high intensity). Additionally, the C=O stretching modes (symmetric at 1543 cm⁻¹ of low IR intensity, asymmetric at 1531 and 1527 cm⁻¹ of high IR intensity) coupled with C–N stretches are the most intense bands. A broad band around 1440 cm⁻¹ comprises many greatly extended vibrations including ring stretching and CH₂ deformation modes.

The calculated spectrum of **H₃15^{Me}** shows C=C stretching vibrations in the range 1620 to 1480 cm⁻¹ with two bands of highest energy at 1632 and 1619 cm⁻¹ being the strongest (Fig. 6c). Below that region, a multitude of very low-intensity vibrations composed of CH₂ deformation modes occur. At 1385 and 1380 cm⁻¹ two moderately intense vibrations with C–O and C–C character are observed. Well defined C–O stretches cannot be assigned. These results allow the assignment of the experimental spectrum of **H₃15^{nBu}**: 1632 cm⁻¹ C=C ring stretching mode, bands around

1456, 1416, and 1379 cm^{-1} mainly composed of CH deformation modes.

Analysis and Discussion

The results section clearly establishes that the chosen DFT method is appropriate to reproduce the experimentally determined molecular structures and the IR spectra. This positive evaluation provides strong confidence that the calculated electronic structures are a good description for these molecules. Thus, we will use the calculated data to analyze some trends in the bonding and how these are reflected in the IR spectra.

Bonding variation as a function of substitution pattern

The monosubstituted benzene derivatives **1**–**5** exhibit an almost unaffected mean $\text{C}^{\text{ar}}\text{--C}^{\text{ar}}$ value of 1.40 Å. The occurrence of a hydroxy and a carbonyl group in *ortho*-position in **H6** and **H7** increases the mean $\text{C}^{\text{ar}}\text{--C}^{\text{ar}}$ value only slightly to 1.41 Å, which by itself does not allow to conclude on a variation of the electronic structure. But the standard deviation of the mean $\text{C}^{\text{ar}}\text{--C}^{\text{ar}}$ bond length increases strongly from 0.003 Å (**2** and **H3**) and 0.007 Å (**4** and **5**) to 0.019 Å (**H6**) and 0.022 Å (**H7**). Moreover, the $\text{C}^{\text{ar}}\text{--C}^{\text{ar}}$ bond between the substituents in **H6** and **H7** is significantly increased (1.43 Å). This perturbation of the benzene ring is well reflected by the HOMA values decreasing from 0.97 for benzene **1** to 0.85 for **H7** (Table 1).

The C–O bonds in **H6** and **H7** (1.34 Å) are shorter than in phenol **H3** (1.38 Å), along with longer C=O bonds (1.24 Å in **H6** vs. 1.22 Å in **4** and 1.25 Å in **H7** vs. 1.23 Å in **5**) and a decrease of the $\text{C}^{\text{ar}}\text{--C}^{\text{C=O}}$ bond length (from 1.48 Å in **4** to 1.45 Å in **H6**, from 1.50 Å in **5** to 1.47 Å in **H7**). These structural features are consistent with main contributions of resonance structure **IX**, but also with some significant contributions of the ionic resonance structure **X** (Scheme 2), which resembles the so-called *ortho*-quinodimethanes [126, 127], and the former may therefore be termed hetero-*ortho*-quinodimethanes.

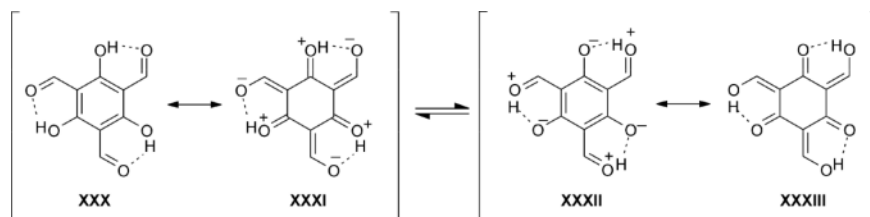
The same effect is observed in aldimine **H8** and ketimine **H9**. The bond length distributions and the HOMA values (0.87 for **H8** and 0.84 for **H9**) of the Schiff bases resemble those of **H6** and **H7** (Table 1). Therefore, the structure of the Schiff bases can be formulated as resonance structure **XIII** with some contributions of the ionic resonance structure **XIV**

Table 1. HOMA values of the geometry-optimized structures of **1**–**H3**, **15**^{Me} and of experimentally determined structures of **H6**_{baron}^{Me} and **H6**_{chand}^{rac}.

Compound	HOMA values
1	0.97
2	0.96
H3	0.96
4	0.95
5	0.95
H6	0.87
H7	0.85
H8	0.87
H9	0.84
H3 10	0.96
H3 11	0.62
H3 12	0.43
H3 13 ^{Me} (enol-imine)	0.64
H3 13 ^{Me} (C _S)	−0.45
H3 13 ^{Me} (C _{3h})	−0.37
H6 _{baron} ^{Me} [51]	−0.28
H3 14 ^{Me}	−0.40
H6 _{chand} ^{rac} [53]	0.08
H3 15 ^{Me}	0.87
[6]radialene [27]	−2.41

(Scheme 2). The stronger proton affinity of amide *versus* alcoholate does not compensate the stabilizing effect of the aromatic ring. Our calculations reproduce the observations which have been made for systems with one RAHB unit fused to an aromatic ring (see Introduction). The results of the calculations do not allow to speculate whether the imine compounds or the carbonyl compounds exhibit more contributions of ionic resonance structure **X** or **XIV**, respectively.

The introduction of three hydroxyl groups in phloroglucinol **H3****10** shows no significant effects concerning the C–O bond length compared to **H3** or the $\text{C}^{\text{ar}}\text{--C}^{\text{ar}}$ bond lengths (Fig. 4) and the HOMA value (0.97 for **1** and 0.96 for **H3****10**) compared to **1**. However, by going from **H3****10** to **H3****11** and **H3****12**, the mean $\text{C}^{\text{ar}}\text{--C}^{\text{ar}}$ bond lengths increase from 1.40 to 1.43 Å. This is corroborated by a decrease of the HOMA values from 0.96 in **H3****10** to 0.62 in **H3****11** and to 0.43 in **H3****12** (Table 1). Moreover, the $\text{C}^{\text{ar}}\text{--O}$ bond lengths decrease in this series from 1.38 to 1.32 Å. This effect is more pronounced than in **H6** and **H7** with mean $\text{C}^{\text{ar}}\text{--C}^{\text{ar}}$ and $\text{C}^{\text{ar}}\text{--O}$ bond lengths of 1.41 and 1.34 Å, respectively. Additionally, the C=O bond length increases from 1.24 (**H6**) to 1.26 Å (**H3****11**) and from 1.25 (**H7**) to 1.27 Å (**H3****12**) accompanied by a decrease of the $\text{C}^{\text{ar}}\text{--C}^{\text{C=O}}$ bond length from 1.45 (**H6**) to 1.44 Å (**H3****11**) and 1.47 (**H7**) to 1.46 Å (**H3****12**).



Scheme 8.

Although the systems with one and with three RAHB systems are in the same phenolic *O*-protonated tautomer, this bond length variation clearly establishes that the ionic resonance structure **XXXI** (Scheme 8) has a larger contribution to the overall resonance structures of **H₃11** and **H₃12** than the ionic resonance structure **X** for the description of **H6** and **H7** (Scheme 2). This trend is corroborated by the HOMA values (Table 1), which show a strong decrease of the aromaticity from 0.87 and 0.85 with one RAHB system (**H6**, **H7**) to 0.62 and 0.43 with three RAHB systems (**H₃11**, **H₃12**). The large contribution of resonance structure **XXXI** indicates that the gain in energy from three RAHB units fused to an aromatic ring almost compensates the gain in energy from aromatic resonance of the benzene ring.

In addition, **H₃11** and **H₃12** exhibit shorter *O*⋯*O* distances (2.49 Å in **H₃11** and 2.40 Å in **H₃12**) and longer *O*–*H* distances (1.05 Å in **H₃11** and 1.09 Å in **H₃12**) than **H6** and **H7** (*O*⋯*O* distances: 2.59 Å in **H6** and 2.53 Å in **H7**; *O*–*H* distances: 1.01 Å in **H6** and 1.02 Å in **H7**), which can be attributed to stronger hydrogen bonds in **H₃11** and **H₃12** than in **H6** and **H7**. Thus, the stronger hydrogen bonds accompanied with π -electron delocalization in **H₃11** and **H₃12** manifest their stronger RAHB than in **H6** and **H7**. The shorter *O*⋯*O* distance in **H₃12** than in **H₃11** might be related to the higher sterical requirements of the methyl groups [128].

It is now interesting to discuss the relative strength of the RAHB in **H₃11** and **H₃12**. The comparison of the structural data of **H6** with **H₃11** and of **H7** and **H₃12** and the much lower HOMA value of **H₃12** (0.43) compared to **H₃11** (0.62), suggest a larger contribution of **XXXI** (Scheme 8) in **H₃12** than in **H₃11**. The shorter *O*⋯*O* distances and longer *O*–*H* distances in **H₃12** than in **H₃11** are also indicative of a stronger hydrogen bond in **H₃12**. According to Gilli [11] a strong π -electron delocalization is indicated if the differences between the *C*–*O**H* and *C*=*O* bond lengths (*q*₁) as well as the *C*=*C* and *C*–*C* bond lengths (*q*₂) are small.

The sum (*Q*) of *q*₁ and *q*₂ should therefore correlate with the strength of the hydrogen bond. This is the case for **H₃11** (*Q* = 0.078, *d*(*O*⋯*O*) = 2.49 Å) and **H₃12** (*Q* = 0.065, *d*(*O*⋯*O*) = 2.40 Å), with **H₃12** exhibiting the stronger RAHB.

The comparison of trialdehyde **H₃11** and trialdimine **H₃13^{Me}** (in the *O*-protonated enol-imine tautomer) shows only minor variations in the mean *C^{ar}*–*C^{ar}* distance (1.43 to 1.42 Å, respectively) and in the *C^{ar}*–*O* distance (1.32 to 1.33 Å, respectively), as well as in the HOMA values (0.62 for **H₃11** and 0.64 for **H₃13^{Me}**, Table 1). The *C^{ar}*–*C^{ar}* distance of 1.44 Å is not affected. Thus, the electronic structure of the hypothetical enol-imine form of **H₃13^{Me}**, *e. g.* the “real” triimine form, closely resembles that of the corresponding aldehyde.

The situation is completely different when considering **H₃13^{Me}** in the energy minimum, *i. e.* the *C*_{3h} symmetric *N*-protonated tautomer. The mean *C^{ar}*–*C^{ar}* bond length increases to 1.46 Å, which is as long as a *C*(*sp*²)–*C*(*sp*²) single bond in conjugated systems [129]. However, this value is still smaller than the bond length in [6]radialenes, *e. g.* 1.51 Å in dodecamethyl[6]radialene [130, 131]. Additionally, the *C*=*O* bond length decreases to 1.27 Å, which reflects a strong *C*=*O* double bond character, comparable to 1.21 Å in cyclic triketones [132]. Also the *C^{ar}*–*C^{CN}* distance of 1.40 Å reflects a strong *C*=*C* double bond character as in dodecamethyl[6]radialene (1.34 Å) [130, 131]. This bond lengths distribution supports resonance structure **XXIX** (Scheme 5) as the main contribution for the description of the electronic structure of **H₃13^{Me}**.

This situation is also reflected in the bond lengths distribution of the triketimine **H₃14^{Me}**, which has the same mean *C^{ar}*–*C^{ar}* bond length of 1.46 Å but a slightly longer *C*=*O* distance (1.28 to 1.27 Å) and a slightly increased *C*–*N* bond length (1.34 to 1.33 Å). Only the *C^{ar}*–*C^{C=N}* distance is significantly longer in **H₃14^{Me}** with 1.43 Å than in **H₃13^{Me}** with 1.40 Å. Importantly,

this effect has also been observed in the experimentally determined solid-state structures.

The HOMA values of $\text{H}_3\mathbf{13}^{\text{Me}}$ and $\text{H}_3\mathbf{14}^{\text{Me}}$ are negative (-0.37 for $\text{H}_3\mathbf{13}^{\text{Me}}$ and -0.40 for $\text{H}_3\mathbf{14}^{\text{Me}}$) demonstrating the loss of a delocalized π system, and support therefore the description of $\text{H}_3\mathbf{13}^{\text{Me}}$ and $\text{H}_3\mathbf{14}^{\text{Me}}$ as heteroradialenes **XXIX** (HOMA value for [6]radialene -2.41 [27]). While for **H8** and **H9** the gain in energy of the resonance of the aromatic ring compensates the gain in energy of one RAHB unit, this is not the case for three such RHAB units. Thus, $\text{H}_3\mathbf{13}^{\text{Me}}$ and $\text{H}_3\mathbf{14}^{\text{Me}}$ are in the *N*-protonated form with loss of the aromaticity in the central aromatic ring. This results in longer O \cdots N distances in $\text{H}_3\mathbf{13}^{\text{Me}}$ compared to **H8** (2.61 and 2.58 Å, respectively), indicative of weaker hydrogen bonds in $\text{H}_3\mathbf{13}^{\text{Me}}$. However, **H9** and $\text{H}_3\mathbf{14}^{\text{Me}}$ exhibit nearly the same O \cdots N distances (2.51 and 2.49 Å, respectively) that are shorter than for **H8** and $\text{H}_3\mathbf{13}^{\text{Me}}$. This shorter O \cdots N distance in $\text{H}_3\mathbf{14}^{\text{Me}}$ might be attributed to the steric demand of the methyl groups [128] which enforces a shorter distance as in **H9** although the hydrogen bond strength should be reduced in the *N*-protonated tautomer.

The effect of hydrogen bonding on the bond lengths distribution is nicely visualized in the C_S symmetric *N*-protonated form of $\text{H}_3\mathbf{13}^{\text{Me}}$. The C=O bond length without hydrogen bond is 1.25 Å, which increases to 1.27 Å for the C=O group with one N–H hydrogen bond donor and to 1.29 Å for the C=O group with two N–H hydrogen bond donors. This effect is propagated to the C^{ar}–C^{ar} distances, which are the longest near the C=O unit without hydrogen bonding (1.48 and 1.47 Å), medium for the C=O group with one hydrogen bond (1.47 and 1.45 Å), and smallest near the C=O group involved in two hydrogen bonds (1.45 Å). These relatively strong effects allow an assignment of the ^1H and ^{13}C resonances of the C_S isomer of $\text{H}_3\mathbf{13}^{\text{nBu}}$ (Scheme 7).

IR spectroscopy as an experimental probe for bonding variations

It is now interesting to analyze how these differences in the electronic structure of the central backbone are reflected in the IR spectra. The shift of the O–H stretch to lower energies from 3600 cm^{-1} in phenol **H3** reflects nicely the trend of the strengths in RAHB: 3011 cm^{-1} in salicylaldehyde **H6**, 2887 cm^{-1} in hydroxyacetophenone **H7**, 2702 cm^{-1} in aldimine

H8, and 2390 cm^{-1} in ketimine **H9**. The strong shifts to lower energy for $\text{H}_3\mathbf{11}$ (2440 cm^{-1}) and $\text{H}_3\mathbf{12}$ (2030 cm^{-1}) confirm the increase of the RAHB in the systems with three RAHB units. The proton transfer in $\text{H}_3\mathbf{13}^{\text{Me}}$ and $\text{H}_3\mathbf{14}^{\text{Me}}$ reduces the hydrogen bonding which is reflected in an increase of $\nu(\text{O-H})$ to 3060 and 2750 cm^{-1} , respectively.

The effect of the hydrogen bonding is also manifested in the C=O stretching frequency, which is shifted from 1708 cm^{-1} in benzaldehyde **4** to 1639 cm^{-1} in salicylaldehyde **H6**, and from 1681 cm^{-1} in acetophenone **5** to 1625 cm^{-1} in hydroxyacetophenone **H7**. The substitution of the carbonyl groups by imine groups leads to a slight shift to lower energies: C=O stretch in salicylaldehyde **H6** at 1638 cm^{-1} vs. C=N stretch in aldimine **H8** at 1630 cm^{-1} , and C=O stretch in hydroxyacetophenone **H7** at 1625 cm^{-1} vs. C=N stretch in ketimine **H9** at 1604 cm^{-1} . There is a gradual change from mainly C=O stretching character in **4** and **5**, to more and more ring stretching character being mixed in on going from **H6** to **H8**, to even mainly ring stretching character in **H9**. Whereas the O–H and C=O/N stretches are decreased in energy by hydrogen bonding, the phenolic C–O stretch increases in energy from 1244 cm^{-1} in phenol **H3** to 1292 and 1305 cm^{-1} in salicylaldehyde **H6** and hydroxyacetophenone **H7**, respectively. The same trend is found in aldimine **H8** (1285 cm^{-1}) and ketimine **H9** (1311 cm^{-1}). These trends of the vibrations reflect well the electronic structure (Scheme 2) discussed above. The fact that the difference of the energy of the C=C and C=O/N stretching modes decreases from **H6** to **H9** is indicative of an increase of the contribution of the resonance structures **X** and **XIV**, respectively.

Figure 7 compares the 1750–1350 cm^{-1} region of the disubstituted *ortho*-carbonylphenol and *ortho*-Schiff base derivatives to its triply extended six-fold substituted analogs. Much stronger intensities of the vibrations of the six-fold substituted species are apparent.

Salicylaldehyde **H6** has an absorption maximum at 1637 cm^{-1} (mainly C=O stretching contribution) with a shoulder at 1572 cm^{-1} (mainly ring stretching contributions). The appearance of the IR spectrum of trialdehyde $\text{H}_3\mathbf{11}$ is almost the same with a maximum at 1638 cm^{-1} and a shoulder at 1585 cm^{-1} , but the origin of the bands is reversed: mainly ring stretches at 1638 cm^{-1} and C=O stretches of minor intensity at 1585 cm^{-1} (Fig. 7a).

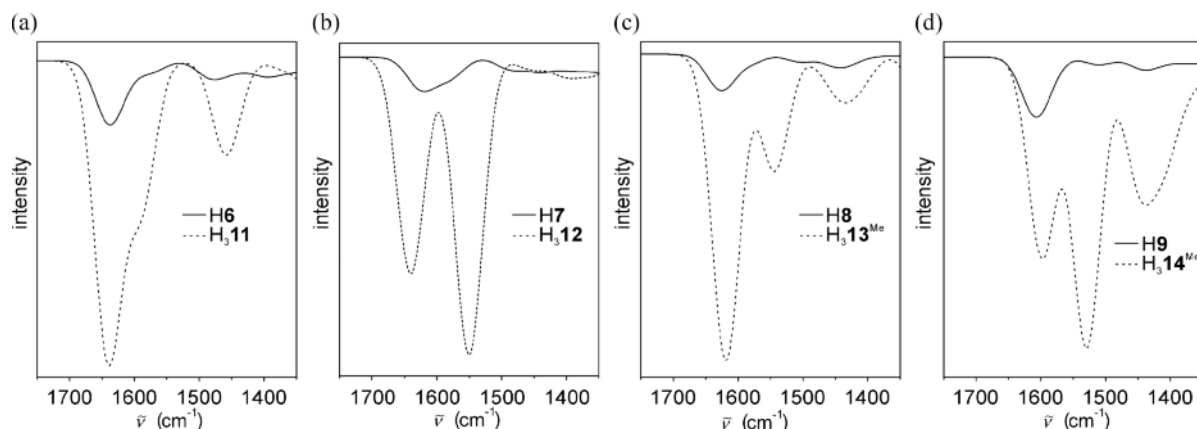


Fig. 7. Comparison of calculated IR spectra of disubstituted and the respective six-fold substituted benzene derivatives: a) H6 vs. H₃11, b) H7 vs. H₃12, c) H8 vs. H₃13^{Me}, d) H9 vs. H₃14^{Me}.

This observation is even more pronounced in the aldimine derivatives of these two aldehydes. The aldimine H8 has a broad asymmetric band with a maximum at 1625 cm⁻¹ with mainly C=N stretching contribution at the high energy side and mainly ring stretching contributions at the lower energy side. In contrast, the strong maximum at 1619 cm⁻¹ of H₃13^{Me} consists mainly of stretching modes of the exocyclic C=C bonds of this heteroradialene, and of a separated maximum at 1544 cm⁻¹ containing mainly C=O stretching modes (Fig. 7c).

This trend in the aldehydes/aldimines is also observed in the ketones/ketimines. Hydroxyacetophenone H7 shows a maximum at 1620 cm⁻¹ (Fig. 7b) for the C=O stretch and a shoulder of mainly ring stretch contributions at 1573 cm⁻¹. In the triketone H₃12 two maxima are apparent at 1640 and 1550 cm⁻¹, both of combined C=O and C=C stretching contributions.

In ketimine H9, one maximum at 1607 cm⁻¹ (Fig. 7d) is observed consisting of C=C and C=N stretching modes. All these trends are manifested in the IR spectrum of the “triketimine” H₃14^{Me} (Fig. 7d). The maximum at 1597 cm⁻¹ consists of mainly stretching modes of the exocyclic C=C double bonds and the higher intensity maximum at 1529 cm⁻¹ of C=O stretching modes.

In the tricarbonyl derivatives H₃11 and H₃12 the C=O and C=C stretching modes are already strongly mixed due to the non-negligible heteroradialene character XXXI (Scheme 8). The main difference to the trialdehyde is a reversed intensity of the two bands with the lower energy (1550 cm⁻¹) band of the trike-

tone H₃12 being strongest, while the higher energy (1638 cm⁻¹) band of the trialdehyde H₃11 is the strongest (Fig. 6a). The better separation of C=C and C=O bands for H₃13^{Me} and H₃14^{Me} compared to that of the trialdehyde H₃11 and the triketone H₃12 reflects the stronger contribution of the heteroradialene resonance structure XXIX (Scheme 5) in H₃13^{Me} and H₃14^{Me} compared to that of XXXI (Scheme 8) in H₃11 and H₃12.

It is now interesting to compare the IR spectra of the heteroradialenes H₃13^{Me} and H₃14^{Me} directly (Fig. 6c). Both consist of three bands in the 1700–1400 cm⁻¹ region. The high energy bands (1619 cm⁻¹ for H₃13^{Me}, 1597 cm⁻¹ for H₃14^{Me}) are assigned to the stretching modes of the exocyclic C=C bonds and the medium energy bands (1544 cm⁻¹ in H₃13^{Me}, 1529 cm⁻¹ in H₃14^{Me}) to the C=O stretches. Ketimine C=N vibrations are usually shifted by 15–20 cm⁻¹ in comparison to those of aldimines induced by the additional CH₃ group. Although H₃13^{Me} and H₃14^{Me} are not imines XXVI but heteroradialenes XXIX (Scheme 5), the same shift is observed by introduction of the CH₃ group in H₃14^{Me}. Besides this energy shift, the intensity ratio of these two bands is reversed (Fig. 6c). Both compounds possess a broad band around 1440 cm⁻¹ consisting of several vibrational modes of ring stretching and C–H bending character.

These calculated IR signatures are well reflected in the experimental spectra. Figure 8a summarizes the spectra of the trialdehyde-based heteroradialenes H₃felden, H₃felddien, H₆feld^{Me} and H₆baron^{Br}. The

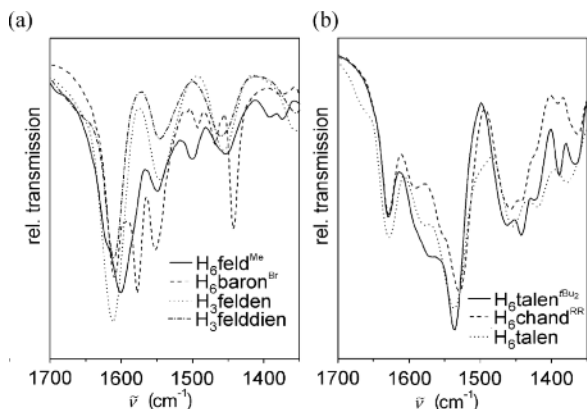


Fig. 8. IR spectroscopic signatures of heteroradialenes: a) experimental IR spectra of $H_3felden$, $H_3felddien$, H_6feld^{Me} and H_6baron^{Br} ; b) experimental IR spectra of H_6talen , $H_6talen^{nBu_2}$, and H_6chand^{RR} .

above discussion allows the assignment of the bands at 1611, 1553 and 1460 cm^{-1} to the heteroradialene backbone, while the bands at 1620 and 1578 cm^{-1} in H_6feld^{Me} and H_6baron^{Br} are assigned to ring stretching modes of the terminal phenolimine units [50, 51]. The same holds true for the triketone-based heteroradialenes H_6talen , $H_6talen^{nBu_2}$, and H_6chand^{RR} (Fig. 8b). A definite assignment of the exocyclic $C=C$ stretching modes to the band at 1590 cm^{-1} and of the $C=O$ stretching modes to that at 1535 cm^{-1} can be made. The bands around 1450 cm^{-1} represent the third typical heteroradialene vibrations consisting of ring stretching and CH bending modes.

One may propose to use the exocyclic $C=C$ stretch and the $C=O$ stretch for the detection of the heteroradialene structure in transition metal complexes. The calculated IR spectra of the reduced H_315^{Me} (Fig. 6c) and the different tautomers of H_313^{Me} (Fig. 6b) all exhibit a band around 1620 cm^{-1} . This band is assigned to a $C=N$ and $C=C$ stretch for H_315^{Me} and for the enolimine tautomer of H_313^{Me} while it is assigned to an exocyclic $C=C$ stretch for the heteroradialene H_313^{Me} (Fig. 6c). Thus, this band is not suitable as a definitive signature. However, only the IR spectrum of H_313^{Me} in the heteroradialene form exhibits a band at 1544 cm^{-1} which is assigned to the $C=O$ stretch. This band will show a shift to lower energy the more the heteroradialene character of the ligand in the complex decreases and therefore allows us to estimate how strong the contribution of the heteroradialene structure is in the complexes.

Recovering of the aromatic character in extended phloroglucinol ligands

In order to recover the aromatic character in our extended phloroglucinol ligands, which is reduced due to heteroradialene resonance structures **XXIX** (Scheme 5), we exchanged the imino by amino groups. The substitution of the imino groups in H_313^{Me} and H_314^{Me} by amino groups in H_315^{Me} has strong implications regarding the electronic structure. The $C^{ar}-C^{ar}$ distance of 1.41 \AA , compared to 1.46 \AA in H_313^{Me} and H_314^{Me} , is a clear indication for the existence of an aromatic character of the central ring, although the mean bond length is slightly larger than 1.40 \AA in phenol **H3** or phloroglucinol **H310**, and the HOMA value (0.87) is lower than for **H3** (0.96) and **H310** (0.96). The long mean $C-O$ bond length of 1.37 \AA compared to the $C=O$ bond length of 1.27 \AA in H_313^{Me} and H_314^{Me} clearly establishes single-bond character, although the value of 1.38 \AA in phenol **H3** and **H310** is slightly longer. However, these deviations can simply be attributed to normal $O-H\cdots N$ hydrogen bonding: the mean $C-O$ bond length of 1.37 \AA in H_315^{Me} is greater than the value of 1.34 \AA in **H8** and **H9** and may be attributed to the difference of a resonance-assisted hydrogen bond and a not resonance-assisted hydrogen bond. The $C^{ar}-C(sp^3)$ bond length of 1.51 \AA perfectly matches the value for a $C^{ar}-C(sp^3)$ single bond of 1.51 \AA [129].

Also the absence of absorption maxima characteristic for our heteroradialene ligands in the UV/Vis spectrum of H_315^{nBu} at $29\,660$ and $33\,910\text{ cm}^{-1}$ reveals the aromatic character of the central ring (Fig. 3). This implies that H_315^R ($R = Me, nBu$) can simply be described as a six-fold substituted benzene ring with a delocalized π system in contrast to the cross-conjugated heteroradialene description for H_313^{Me} and H_314^{Me} .

The substitution of the three imine groups in H_313^{Me} by three amine groups in H_315^{Me} results in significant differences in the IR spectrum (Fig. 6c). Instead of the two characteristic bands at 1619 and 1544 cm^{-1} for H_313^{Me} , H_315^{Me} shows only one band at 1628 cm^{-1} of benzene-typical ring-stretching character.

Conclusions

We have calculated the molecular structures and IR spectra of the benzene derivatives **1** to H_315^{Me} . The

comparison of these calculated data with those of experimentally determined molecular structures and IR spectra has confirmed that the chosen DFT method is well suited to establish the electronic structure of this series of benzene derivatives.

The RAHB in the *ortho*-carbonylphenols **H6** and **H7** and in the *ortho*-Schiff bases **H8** and **H9** reduces slightly the aromatic character in comparison to the mono-substituted analogs **H3–5** providing some *ortho*-quinodimethane character. These trends are nicely reflected in the IR spectra by a decrease of the energy of the O–H and C=O/C=N stretches, and by an increase in the energy of the C–O stretch. The presence of three RAHB systems in the trialdehyde **H311** and the triketone **H312** results in a stronger heteroradialene character, the reduction of the aromaticity by the RAHB in **H312** being stronger than in **H311**. However, the gain in energy by the resonance of the aromatic ring is still large, but close to the gain in energy by the resonance of three RAHB units fused to the aromatic ring.

This behavior changes for the triimines **H313^{Me}** and **H314^{Me}** where the gain in energy by the resonance of the three RAHB units exceeds the aromatic stabilization so that proton transfer occurs, leading to **H313^{Me}** and **H314^{Me}** as the *N*-protonated tautomers. These are best described by a heteroradialene resonance structure accompanied by the loss of the aromatic character of the central ring.

The increase of RAHB from **H6** to **H312** and the heteroradialene formation in **H313^{Me}** and **H314^{Me}** are well reflected in the IR spectra. The “usual” feature of a strong C=O/C=N stretching mode in the 1600–1650 cm⁻¹ region accompanied by a lower energy and lower intensity ring stretching mode as observed in **H6** and **H8** is disturbed in such a way that the C=O/C=N stretch and the ring stretches mix causing a low-energy shift of the C=O/C=N stretch and a high energy shift of the ring stretch. This culminates in the heteroradialenes with the C=C stretches of the exocyclic double bonds giving rise to the strongest band in the 1600–1650 cm⁻¹ region and C=O stretches of lower intensity around 1550 cm⁻¹.

These observations allow an assignment of the experimental IR spectra of our extended phloroglucinol ligands identifying them as compounds with characteristic features of heteroradialenes. The bands at 1611 and 1553 cm⁻¹ in the trialdehyde-based ligands are assigned to C=C stretches of the exocyclic double bonds and to C=O stretches, respectively. For the triketone-

based ligands these bands are shifted to 1590 and 1535 cm⁻¹, respectively. The C=O band might be suitable as a signature for the detection of the heteroradialene character of our ligands in transition metal complexes.

The substitution of the three imino groups in **H313^R** (R = Me, *n*Bu) by amino groups in **H315^R** (R = Me, *n*Bu) recovers the aromatic character of the central benzene ring, because a resonance between the hydrogen bond donor and acceptor is simply not possible. Therefore this substitution serves as a new *leitmotiv* for the rational improvement of our ligand systems to strengthen the exchange coupling in our complexes.

Experimental Section

Preparation of compounds

Compounds **1–H6**, **H310**, solvents, and starting materials were of the highest commercially available purity and used as received. 2,4,6-Triformylphloroglucinol (**H311**) [30] and 2,4,6-triacetylphloroglucinol (**H312**) [133] were prepared according to reported procedures. The assignments of the NMR resonances (Scheme 7) in all products were supported by 2D COSY, HMBC, and HMQC spectroscopy.

2,4,6-Tris[(butylimino)methyl]-1,3,5-trihydroxybenzene (**H313^{nBu}**)

H313^{nBu} was synthesized by using a modified literature protocol [85] and characterized completely herein. To a suspension of **H311** (62 mg, 0.23 mmol) and sodium sulfate in dichloromethane (10 mL) was added a solution of butylamine (90 mg, 1.23 mmol) in dichloromethane (2 mL). The mixture was stirred for 7 h at room temperature. After filtration the volatiles were removed *in vacuo* which afforded **H313^{nBu}** as a yellow highly viscous oil. Yield: 99 mg (89%). – IR (KBr): $\nu = 1611\text{s}, 1547\text{s}, 1452\text{s}, 1325\text{m}, 1288\text{m}, 1252\text{m}, 1209\text{m}, 1144\text{m}, 739\text{w cm}^{-1}$. – ¹H NMR (500.25 MHz, CDCl₃): $\delta = 11.40$ (m, N(4a)H + N(4b)H), 10.95 (m, N(4c)H + N(4d)H), 8.24 (d, ³J(H,H) = 13.6 Hz, HC(3b)N), 8.22 (d, ³J(H,H) = 13.6 Hz, HC(3c)N), 8.14 (d, ³J(H,H) = 13.6 Hz, HC(3a)N), 8.10 (d, ³J(H,H) = 13.6 Hz, HC(3d)N), 3.39 (m, C(5a-d)H₂), 1.62 (m, C(6a-d)H₂), 1.39 (m, C(7a-d)H₂), 0.93 (m, C(8a-d)H₃) ppm. – ¹³C NMR (125.75 MHz, CDCl₃): $\delta = 188.1$ (C-1c), 185.4 (C-1b), 185.36 (C-1a), 182.8 (C-1d), 158.3 (C-3d), 157.8 (C-3c), 157.3 (C-3a), 156.6 (C-3b), 104.7 (C-2b), 104.6 (C-2c), 104.5 (C-2a), 104.4 (C-2d), 50.01, 49.96 (br, C-5a-c), 32.9, 32.8, 32.7 (br, C-6a-c), 19.8 (br, C-7a-c), 13.8, 13.7, 13.6 (br, C-8a-d) ppm. – ESI-MS (CHCl₃/MeOH): $m/z = 376.2$ [M+H]⁺, 398.2 [M+Na]⁺. – C_{21.55}H_{34.1}N₃O₃Cl_{1.1} (**H313^{nBu}**·0.55CH₂Cl₂, 422.2): calcd. C 61.30, H 8.14, N 9.95; found C 61.30, H 8.41, N 10.16.

Compound	H ₃ 11	H ₃ 12
Empirical formula	C ₉ H ₆ O ₆	C ₁₂ H ₁₂ O ₆
<i>F</i> w, g mol ⁻¹	210.14	252.22
<i>T</i> , K	100(2)	100(2)
Space group	<i>P</i> 6 ₁	<i>P</i> 2 ₁ / <i>c</i>
<i>a</i> , Å	8.7540(2)	9.2700(10)
<i>b</i> , Å	8.7540(2)	16.5880(16)
<i>c</i> , Å	18.3991(4)	7.2331(8)
β, deg	90	106.781(6)
<i>V</i> , Å ³	1221.07(5)	1064.87(19)
<i>Z</i>	6	4
ρ _{calcd} , g cm ⁻³	1.72	1.57
λ, Å / μ, mm ⁻¹	1.54178 / 1.3	0.71073 / 0.1
Crystal size, mm ³	0.25 × 0.21 × 0.14	0.40 × 0.06 × 0.02
Coll. reflns. / 2 θ _{max} , deg	29377 / 69.34	11348 / 24.99
Unique reflns. / <i>R</i> _{int}	1517 / 0.0373	1837 / 0.0781
Obs. reflns. [<i>I</i> > 2σ(<i>I</i>)]	1507	1379
Data / restraints / parameters	1517 / 1 / 139	1837 / 3 / 178
Goodness-of-fit ^a on <i>F</i> ²	1.263	1.038
<i>R</i> 1 ^b / <i>wR</i> 2 ^c [<i>I</i> > 2(<i>I</i>)]	0.0480 / 0.1288	0.0414 / 0.1049
Abs. structure parameter	0.1(4)	–
Max / min residuals, e Å ⁻³	0.33 / –0.29	0.28 / –0.24

Table 2. Crystallographic data for H₃11 and H₃12.

^a GoF = [Σw(*F*_o² – *F*_c²)/(*n*_{obs} – *n*_{param})]^{1/2}; ^b *R*1 = Σ||*F*_o – |*F*_c||/Σ|*F*_o|; ^c *wR*2 = [Σw(*F*_o² – *F*_c²)/Σw(*F*_o²)]^{1/2}, *w* = [σ²(*F*_o²) + (*AP*)² + *BP*]⁻¹, where *P* = (Max(*F*_o², 0) + 2*F*_c²)/3.

2,4,6-Tris[(butyl(methyl)amino)methyl]-1,3,5-trihydroxybenzene (H₃15^{nBu})

A mixture of H₃10 (50 mg, 0.40 mmol), methylbutylamine (138 mg, 1.59 mmol), and formaldehyde in ethanol (6 mL) was stirred over night. The volatiles were removed *in vacuo*, affording H₃15^{nBu} as a yellow oil. Yield: 90 mg (54 %). – IR (KBr) *v* = 2957s, 2934s, 2861s, 2807s, 2699m, 1632s, 1456s, 1416s, 1379s, 1346s, 1277m, 1200m, 1161m, 1140m, 1111s, 1086m, 1059m, 1024m, 990m, 964m, 907m, 889m, 847m, 808m, 750m, 735m, 575m cm⁻¹. – ¹H NMR (500.25 MHz, CDCl₃): δ = 9.03 (s, 3H, OH), 3.70 (s, 6H, C_{Ar}CH₂), 2.47 (m, 6H, NCH₂CH₂), 2.25 (s, 9H, NCH₃), 1.52 (quin, ³*J*(H,H) = 7.4 Hz, 6H, CH₂CH₂CH₂), 1.31 (sext, ³*J*(H,H) = 7.4 Hz, 6H, CH₂CH₂CH₃), 0.98 (t, ³*J*(H,H) = 7.4 Hz, 9H, CH₂CH₃) ppm. – ¹³C NMR (125.75 MHz, CDCl₃): δ = 156.2 (C_{Ar}OH), 99.3 (C_{Ar}CH₂), 56.9 (NCH₂CH₂), 54.1 (C_{Ar}CH₂), 29.3 (CH₂CH₂CH₂), 20.6 (CH₂CH₃), 14.1 ppm (CH₃) ppm. – HRMS (ESI: CHCl₃/MeOH): *m/z* = 424.3529 (calcd. 424.3534 for C₂₄H₄₆N₃O (H₃15^{nBu}), [M+H]⁺).

X-Ray crystallography

Single crystals of trialdehyde H₃11 and triketone H₃12 were grown from chloroform solutions, coated with oil, and measured at 100 K on a Bruker X8-Prospector diffractometer (three circle goniometer, CuK_α radiation, IμS micro-focus source with multilayer optics) and a Bruker Kappa

ApexII diffractometer (four-circle goniometer, MoK_α radiation, focussing graphite monochromator), respectively, using ω- and φ-scans. Empirical absorption corrections using equivalent reflections were performed with the program SADABS [134]. The structures were solved with the program SHELXS-97 [135] and refined using SHELXL-97 [135]. Crystal data and further details concerning the crystal structure determination are found in Table 2.

CCDC 884775 (H₃12) and CCDC 884776 (H₃11) contain the supplementary crystallographic data for this paper. These data can be obtained free of charge from The Cambridge Crystallographic Data Centre via www.ccdc.cam.ac.uk/data_request/cif.

Other physical measurements

Infrared spectra (400–4000 cm⁻¹) of solid samples were recorded from KBr disks and that of liquid compounds from films on KBr disks on a Shimadzu FTIR-8400S spectrometer. UV/Vis/NIR absorption spectra of solutions were measured on a Shimadzu UV-3101PC spectrophotometer in the range of 200–1200 nm at ambient temperatures. ESI mass spectra were recorded on a Bruker Esquire 3000 ion trap mass spectrometer equipped with a standard ESI source. Accurate mass was measured on a Thermo Scientific Orbitrap LTQ XL with external calibration. ¹H and ¹³C NMR spectra were measured on a Bruker DRX500 spectrometer using the solvent as an internal standard.

Computational details

Theoretical calculations were based on Density Functional Theory (DFT) and performed with the ORCA program package [136]. The geometry optimization and frequency calculations were carried out using the BP86 [137–139] functional in combination with the triple-zeta quality TZVP basis set [140, 141]. An auxiliary basis set TZV/J was employed for the RI approximation [142–144]. Tight SCF con-

vergence criteria were used. Vibrational frequencies were calculated by numerical differentiation of analytic gradients with a displacement value of 0.001 Å.

Acknowledgement

This work was supported by the DFG (FOR945 “Nanomagnets: from Synthesis *via* Interactions with Surfaces to Function”), the Fonds der Chemischen Industrie, and Bielefeld University.

- [1] J. Dabrowski, *Spectrochim. Acta* **1963**, *19*, 475–496.
[2] J. Dabrowski, U. Dabrowska, *Chem. Ber.* **1968**, *101*, 2365–2374.
[3] J. Dabrowski, U. Dabrowska, *Chem. Ber.* **1968**, *101*, 3392–3402.
[4] P. J. Taylor, *Spectrochim. Acta A* **1970**, *26*, 165–194.
[5] D. Smith, P. J. Taylor, *Spectrochim. Acta A* **1976**, *32*, 1477–1488.
[6] U. Dabrowska, J. Dabrowski, *Bull. Chem. Soc. Jpn.* **1975**, *48*, 1014–1017.
[7] D. Smith, P. J. Taylor, *Spectrochim. Acta A* **1976**, *32*, 1489–1502.
[8] N. Taoufik, R. R. Pappalardo, E. Sánchez Marcos, *Chem. Phys. Lett.* **2000**, *323*, 400–406.
[9] S. I. Vdovenko, I. I. Gerus, E. A. Fedorenko, *Spectrochim. Acta A* **2009**, *74*, 1010–1015.
[10] P. Gilli, V. Bertolasi, V. Ferretti, G. Gilli, *J. Am. Chem. Soc.* **2000**, *122*, 10405–10417.
[11] G. Gilli, F. Bellucci, V. Ferretti, V. Bertolasi, *J. Am. Chem. Soc.* **1989**, *111*, 1023–1028.
[12] V. Bertolasi, P. Gilli, V. Ferretti, G. Gilli, *J. Am. Chem. Soc.* **1991**, *113*, 4917–4925.
[13] I. Alkorta, J. Elguero, O. Mó, M. Yáñez, J. E. Del Bene, *Mol. Phys.* **2004**, *102*, 2563–2574.
[14] P. Sanz, O. Mó, M. Yáñez, J. Elguero, *ChemPhys Chem* **2007**, *8*, 1950–1958.
[15] P. Sanz, O. Mó, M. Yáñez, J. Elguero, *J. Phys. Chem. A* **2007**, *111*, 3585–3591.
[16] P. Sanz, O. Mó, M. Yáñez, J. Elguero, *Chem. Eur. J.* **2008**, *14*, 4225–4232.
[17] L. Sobczyk, S. J. Grabowski, T. M. Krygowski, *Chem. Rev.* **2005**, *105*, 3513–3560.
[18] G. Gilli, P. Gilli, *J. Mol. Struct.* **2000**, *552*, 1–15.
[19] P. Lenain, M. Mandado, R. A. Mosquera, P. Bultinck, *J. Phys. Chem. A* **2008**, *112*, 10689–10696.
[20] M. Cuma, S. Scheiner, T. Kar, *J. Mol. Struct. THEOCHEM* **1999**, *467*, 37–49.
[21] K. B. Borisenko, C. W. Bock, I. Hargittai, *J. Phys. Chem.* **1996**, *100*, 7426–7434.
[22] M. Palusiak, S. Simon, M. Solà, *J. Org. Chem.* **2006**, *71*, 5241–5248.
[23] K. B. Borisenko, I. Hargittai, *J. Mol. Struct. THEOCHEM* **1996**, *388*, 107–113.
[24] T. M. Krygowski, *J. Chem. Inf. Comput. Sci.* **1993**, *33*, 70–78.
[25] J. Kruszewski, T. M. Krygowski, *Tetrahedron Lett.* **1972**, *13*, 3839–3842.
[26] H. Houjou, T. Motoyama, S. Banno, I. Yoshikawa, K. Araki, *J. Org. Chem.* **2008**, *74*, 520–529.
[27] T. M. Krygowski, M. K. Cyranski, *Phys. Chem. Chem. Phys.* **2004**, *6*, 249–255.
[28] M. Sauer, C. Yeung, J. H. Chong, B. O. Patrick, M. J. MacLachlan, *J. Org. Chem.* **2006**, *71*, 775–788.
[29] E. S. Aazam, *Acta Crystallogr.* **2007**, *E63*, o2751–o2752.
[30] J. H. Chong, M. Sauer, B. O. Patrick, M. J. MacLachlan, *Org. Lett.* **2003**, *5*, 3823–3826.
[31] J. A. Riddle, S. P. Lathrop, J. C. Bollinger, D. Lee, *J. Am. Chem. Soc.* **2006**, *128*, 10986–10987.
[32] D. Chandran, C. Bae, I. Ahn, C.-S. Ha, I. Kim, *J. Organomet. Chem.* **2009**, *694*, 1254–1258.
[33] X. Jiang, J. C. Bollinger, D. Lee, *J. Am. Chem. Soc.* **2006**, *128*, 11732–11733.
[34] C. V. Yelamaggad, A. S. Achalkumar, D. S. Shankar Rao, S. K. Prasad, *J. Am. Chem. Soc.* **2004**, *126*, 6506–6507.
[35] J. A. Riddle, J. C. Bollinger, D. Lee, *Angew. Chem. Int. Ed.* **2005**, *44*, 6689–6693.
[36] C. V. Yelamaggad, A. S. Achalkumar, D. S. S. Rao, S. K. Prasad, *J. Org. Chem.* **2007**, *72*, 8308–8318.
[37] X. Jiang, M. C. Vieweger, J. C. Bollinger, B. Dragnea, D. Lee, *Org. Lett.* **2007**, *9*, 3579–3582.
[38] X. Jiang, Y.-K. Lim, B. J. Zhang, E. A. Opsitnick, M.-H. Baik, D. Lee, *J. Am. Chem. Soc.* **2008**, *130*, 16812–16822.
[39] C. V. Yelamaggad, A. S. Achalkumar, *Tetrahedron Lett.* **2006**, *47*, 7071–7075.
[40] M. Vieweger, X. Jiang, Y.-K. Lim, J. Jo, D. Lee, B. Dragnea, *J. Phys. Chem. A* **2011**, *115*, 13298–13308.
[41] C. V. Yelamaggad, A. S. Achalkumar, D. S. S. Rao, S. K. Prasad, *J. Mat. Chem.* **2007**, *17*, 4521–4529.

- [42] Y.-K. Lim, X. Jiang, J. C. Bollinger, D. Lee, *J. Mat. Chem.* **2007**, *17*, 1969–1980.
- [43] C. V. Yelamaggad, A. S. Achalkumar, D. S. S. Rao, S. K. Prasad, *J. Org. Chem.* **2009**, *74*, 3168–3171.
- [44] J. A. Riddle, X. Jiang, J. Huffman, D. Lee, *Angew. Chem. Int. Ed.* **2007**, *46*, 7019–7022.
- [45] T. Glaser, M. Gerenkamp, R. Fröhlich, *Angew. Chem. Int. Ed.* **2002**, *41*, 3823–3825.
- [46] B. Feldscher, A. Stammler, H. Bögge, T. Glaser, *Dalton Trans.* **2010**, *39*, 11675–11685.
- [47] B. Feldscher, A. Stammler, H. Bögge, T. Glaser, *Polyhedron* **2011**, *30*, 3038–3047.
- [48] T. Glaser, M. Heidemeier, T. Lügger, *Dalton Trans.* **2003**, 2381–2383.
- [49] T. Glaser, M. Heidemeier, R. Fröhlich, P. Hildebrandt, E. Bothe, E. Bill, *Inorg. Chem.* **2005**, *44*, 5467–5482.
- [50] B. Feldscher, E. Krickmeyer, M. Moselage, H. Theil, V. Hoeke, Y. Kaiser, A. Stammler, H. Bögge, *Sci. China: Chem.* **2012**, *55*, 951–966.
- [51] C.-G. Freiherr von Richthofen, A. Stammler, H. Bögge, T. Glaser, *J. Org. Chem.* **2012**, *77*, 1435–1448.
- [52] C. Mukherjee, A. Stammler, H. Bögge, T. Glaser, *Inorg. Chem.* **2009**, *48*, 9476–9484.
- [53] C. Mukherjee, A. Stammler, H. Bögge, T. Glaser, *Chem. Eur. J.* **2010**, *16*, 10137–10149.
- [54] S. Walleck, H. Theil, M. Heidemeier, G. Heinze-Brückner, A. Stammler, H. Bögge, T. Glaser, *Inorg. Chim. Acta* **2010**, *363*, 4287–4294.
- [55] H. Hopff, A. K. Wick, *Helv. Chim. Acta* **1961**, *44*, 380–386.
- [56] H. Hopf, G. Maas, *Angew. Chem., Int. Ed. Engl.* **1992**, *31*, 931–954.
- [57] H. Hopf, *Classics in Hydrocarbon Chemistry*, Wiley-VCH, New York **2000**, pp. 290–300.
- [58] S. Eisler, R. R. Tykwinski, *Angew. Chem. Int. Ed.* **1999**, *38*, 1940–1943.
- [59] M. Gholami, R. R. Tykwinski, *Chem. Rev.* **2006**, *106*, 4997–5027.
- [60] R. R. Tykwinski, M. Gholami, S. Eisler, Y. Zhao, F. Melin, L. Echegoyen, *Pure Appl. Chem.* **2008**, *80*, 621–637.
- [61] M. Gholami, F. Melin, R. McDonald, M. J. Ferguson, L. Echegoyen, R. R. Tykwinski, *Angew. Chem. Int. Ed.* **2007**, *46*, 9081–9085.
- [62] G. Maas, H. Hopf in *The Chemistry of Dienes and Polyenes*, Vol.1 (Ed.: Z. Rappoport), Wiley, Chichester **1997**, chapter 21, pp. 925–977.
- [63] C.-G. Freiherr von Richthofen, A. Stammler, H. Bögge, T. Glaser, *Eur. J. Inorg. Chem.* **2011**, 49–52.
- [64] T. Glaser, H. Theil, M. Heidemeier, *C. R. Chimie* **2008**, *11*, 1121–1136.
- [65] H. C. Longuet-Higgins, *J. Chem. Phys.* **1950**, *18*, 265–274.
- [66] H. M. McConnell, *J. Chem. Phys.* **1963**, *39*, 1910.
- [67] H. Iwamura, *Adv. Phys. Org. Chem.* **1990**, *26*, 179–253.
- [68] H. Iwamura, N. Koga, *Acc. Chem. Res.* **1993**, *26*, 346–351.
- [69] A. Rajca, *Chem. Eur. J.* **2002**, *8*, 4834–4841.
- [70] K. Yoshizawa, R. Hoffmann, *J. Am. Chem. Soc.* **1995**, *117*, 6921–6926.
- [71] D. A. Dougherty, *Acc. Chem. Res.* **1991**, *24*, 88–94.
- [72] A. A. Ovchinnikov, *Theoret. Chim. Acta* **1978**, *47*, 297–304.
- [73] P. Karafiloglou, *J. Chem. Phys.* **1985**, *82*, 3728–3740.
- [74] M. Okamoto, Y. Teki, T. Takui, T. Kinoshita, K. Itoh, *Chem. Phys. Lett.* **1990**, *173*, 265–270.
- [75] J. Cano, E. Ruiz, S. Alvarez, M. Verdaguier, *Comm. Inorg. Chem.* **1998**, *20*, 27–56.
- [76] F. Lloret, G. De Munno, M. Julve, J. Cano, R. Ruiz, A. Caneschi, *Angew. Chem. Int. Ed.* **1998**, *37*, 135–138.
- [77] X. Ottenwaelder, J. Cano, Y. Journaux, E. Riviere, C. Brennan, M. Nierlich, R. Ruiz-Garcia, *Angew. Chem. Int. Ed.* **2004**, *43*, 850–852.
- [78] I. Fernández, R. Ruiz, J. Faus, M. Julve, F. Lloret, J. Cano, X. Ottenwaelder, Y. Journaux, C. Munoz, *Angew. Chem. Int. Ed.* **2001**, *40*, 3039–3042.
- [79] E. Pardo, R. Ruiz-Garcia, J. Cano, X. Ottenwaelder, R. Lescouezec, Y. Journaux, F. Lloret, M. Julve, *Dalton Trans.* **2008**, 2780–2805.
- [80] T. Glaser, *Chem. Commun.* **2011**, *47*, 116–130.
- [81] I. E. Serdiuk, M. Wera, A. D. Roshal, P. Sowinski, B. Zadykowicz, J. Blazejowski, *Tetrahedron Lett.* **2011**, *52*, 2737–2740.
- [82] P. Suresh, S. Srimurugan, B. Babu, H. N. Pati, *Tetrahedron: Asymmetry* **2007**, *18*, 2820–2827.
- [83] Y.-K. Lim, S. Wallace, J. C. Bollinger, X. Chen, D. Lee, *Inorg. Chem.* **2007**, *46*, 1694–1703.
- [84] R. M. Claramunt, C. López, M. D. Santa María, D. Sanz, J. Elguero, *Prog. Nuc. Magn. Reson. Spec.* **2006**, *49*, 169–206.
- [85] J. Leclaire, G. Husson, N. Devaux, V. Delorme, L. Charles, F. Ziarelli, P. Desbois, A. Chaumonnot, M. Jacquin, F. Fotiadu, G. Buono, *J. Am. Chem. Soc.* **2010**, *132*, 3582–3593.
- [86] J. D. Pettigrew, P. D. Wilson, *J. Org. Chem.* **2006**, *71*, 1620–1625.
- [87] D. J. Tozer, *J. Chem. Phys.* **1996**, *104*, 4166–4172.
- [88] N. C. Handy, C. W. Murray, R. D. Amos, *J. Phys. Chem.* **1993**, *97*, 4392–4396.
- [89] N. C. Handy, P. E. Maslen, R. D. Amos, J. S. Andrews, C. W. Murray, G. J. Laming, *Chem. Phys. Lett.* **1992**, *197*, 506–515.
- [90] E. Albertazzi, F. Zerbetto, *Chem. Phys.* **1992**, *164*, 91–97.

- [91] A. Bérces, T. Ziegler, *J. Chem. Phys.* **1993**, *98*, 4793–4804.
- [92] B. Galabov, S. Ilieva, T. Gounev, D. Steele, *J. Mol. Struct.* **1992**, *273*, 85–98.
- [93] G. Keresztury, F. Billes, M. Kubinyi, T. Sundius, *J. Phys. Chem. A* **1998**, *102*, 1371–1380.
- [94] A. Mukherjee, M. L. McGlashen, T. G. Spiro, *Journal of Physical Chemistry* **1995**, *99*, 4912–4917.
- [95] D. Michalska, D. C. Bienko, A. J. Abkowicz-Bienko, Z. Latajka, *J. Phys. Chem.* **1996**, *100*, 17786–17790.
- [96] J. Palomar, J. L. G. De Paz, J. Catalán, *Chem. Phys.* **1999**, *246*, 167–208.
- [97] V. Schreiber, S. Melikova, K. Rutkowski, D. Shchepkin, A. Shurukhina, A. Koll, *J. Mol. Struct.* **1996**, *381*, 141–148.
- [98] H. Lampert, W. Mikenda, A. Karpfen, *J. Phys. Chem. A* **1997**, *101*, 2254–2263.
- [99] A. Filarowski, A. Koll, P. Lipkowski, A. Pawlukojé, *J. Mol. Struct.* **2008**, *880*, 97–108.
- [100] M. Spoliti, L. Bencivenni, J. J. Quirante, F. Ramondo, *J. Mol. Struct. THEOCHEM* **1997**, *390*, 139–148.
- [101] K. Tamagawa, T. Iijima, M. Kimura, *J. Mol. Struct.* **1976**, *30*, 243–253.
- [102] G. E. Bacon, N. A. Curry, S. A. Wilson, *Proc. R. Soc. London, Ser. A* **1964**, *279*, 98–110.
- [103] R. Seip, G. Schultz, I. Hargittai, Z. G. Szabo, *Z. Naturforsch.* **1977**, *32a*, 1178–1183.
- [104] A. Domenicano, G. Schultz, M. Kolonits, I. Hargittai, *J. Mol. Struct.* **1979**, *53*, 197–209.
- [105] M. Anderson, L. Bosio, J. Bruneauxpouille, R. Fourme, *J. Chim. Phys. Phys. – Chim. Biol.* **1977**, *74*, 68–73.
- [106] G. Portalone, G. Schultz, A. Domenicano, I. Hargittai, *Chem. Phys. Lett.* **1992**, *197*, 482–488.
- [107] D. R. Allan, S. J. Clark, A. Dawson, P. A. McGregor, S. Parsons, *Acta Crystallogr.* **2002**, *B58*, 1018–1024.
- [108] Y. Tanimoto, H. Kobayashi, S. Nagakura, Y. Saito, *Acta Crystallogr.* **1973**, *B29*, 1822–1826.
- [109] P. Talukder, S. Shit, A. Sasmal, S. R. Batten, B. Mobaraki, K. S. Murray, S. Mitra, *Polyhedron* **2011**, *30*, 1767–1773.
- [110] A. Filarowski, T. Glowia, A. Koll, *J. Mol. Struct.* **1999**, *484*, 75–89.
- [111] C. H. Gorbitz, M. Kaboli, M. L. Read, K. Vestli, *Acta Crystallogr.* **2008**, *E64*, o2023.
- [112] J. Abildgaard, S. Bolvig, P. E. Hansen, *J. Am. Chem. Soc.* **1998**, *120*, 9063–9069.
- [113] A. Mukherjee, M. L. McGlashen, T. G. Spiro, *J. Phys. Chem.* **1995**, *99*, 4912–4917.
- [114] H. D. Bist, J. C. D. Brand, D. R. Williams, *J. Mol. Spectrosc.* **1967**, *24*, 402–412.
- [115] J. C. Evans, *Spectrochim. Acta* **1960**, *16*, 1382–1392.
- [116] T. Glaser, M. Heidemeier, S. Grimme, E. Bill, *Inorg. Chem.* **2004**, *43*, 5192–5194.
- [117] T. Glaser, M. Heidemeier, J. B. H. Strautmann, H. Bögge, A. Stämmler, E. Krickemeyer, R. Huenerbein, S. Grimme, E. Bothe, E. Bill, *Chem. Eur. J.* **2007**, *13*, 9191–9206.
- [118] T. Glaser, M. Heidemeier, R. Fröhlich, *C. R. Chimie* **2007**, *10*, 71–78.
- [119] T. Glaser, M. Heidemeier, T. Weyhermüller, R.-D. Hoffmann, H. Rupp, P. Müller, *Angew. Chem. Int. Ed.* **2006**, *45*, 6033–6037.
- [120] T. Glaser, M. Heidemeier, E. Krickemeyer, H. Bögge, A. Stämmler, R. Fröhlich, E. Bill, J. Schnack, *Inorg. Chem.* **2009**, *48*, 607–620.
- [121] T. Glaser, M. Heidemeier, H. Theil, A. Stämmler, H. Bögge, J. Schnack, *Dalton Trans.* **2010**, *39*, 192–199.
- [122] C.-G. Freiherr von Richthofen, A. Stämmler, H. Bögge, M. W. DeGroot, J. R. Long, T. Glaser, *Inorg. Chem.* **2009**, *48*, 10165–10176.
- [123] D. Plaul, W. Plass, *Inorg. Chim. Acta* **2011**, *374*, 341–349.
- [124] H. Theil, C.-G. Freiherr von Richthofen, A. Stämmler, H. Bögge, T. Glaser, *Inorg. Chim. Acta* **2008**, *361*, 916–924.
- [125] E. Krickemeyer, V. Hoeke, A. Stämmler, H. Bögge, J. Schnack, T. Glaser, *Z. Naturforsch.* **2010**, *65b*, 295–303.
- [126] J. L. Segura, N. Martín, *Chem. Rev.* **1999**, *99*, 3199–3246.
- [127] J. L. Charlton, M. M. Alauddin, *Tetrahedron* **1987**, *43*, 2873–2889.
- [128] A. Filarowski, A. Koll, T. Glowiak, *J. Chem. Soc., Perkin Trans.* **2002**, 835–842.
- [129] F. H. Allen, O. Kennard, D. G. Watson, L. Brammer, A. G. Orpen, R. Taylor, *J. Chem. Soc., Perkin Trans. 2*, **1987**, S1–S19.
- [130] T. Höpfner, P. G. Jones, B. Ahrens, I. Dix, L. Ernst, H. Hopf, *Eur. J. Org. Chem.* **2003**, 2596–2611.
- [131] G. Wilke, *Angew. Chem., Int. Ed. Engl.* **1988**, *27*, 185–206.
- [132] H. M. R. Hoffmann, U. Eggert, A. Walenta, E. Weineck, D. Schomburg, R. Wartchow, F. H. Allen, *J. Org. Chem.* **1989**, *54*, 6096–6100.
- [133] H. Friese, *Chem. Ber.* **1931**, *64*, 2109–2112.
- [134] G. M. Sheldrick, SADABS, University of Göttingen, Göttingen (Germany) **2008**.
- [135] G. M. Sheldrick, *Acta Crystallogr.* **2008**, *A64*, 112–122.
- [136] F. Neese, ORCA – An ab initio, Density Functional and Semiempirical Program Package (v. 2.8–20) University of Bonn, Bonn (Germany) **2010**.
- [137] A. D. Becke, *Phys. Rev. A* **1988**, *38*, 3098–3100.

- [138] J. P. Perdew, *Phys. Rev. B* **1986**, *33*, 8822–8824.
- [139] J. P. Perdew, *Phys. Rev. B* **1986**, *34*, 7406.
- [140] A. Schäfer, C. Huber, R. Ahlrichs, *J. Chem. Phys.* **1994**, *100*, 5829–5835.
- [141] A. Schäfer, H. Horn, R. Ahlrichs, *J. Chem. Phys.* **1992**, *97*, 2571–2577.
- [142] A. Weigend, *Phys. Chem. Chem. Phys.* **2006**, *8*, 1057–1065.
- [143] K. Eichkorn, O. Treutler, H. Öhm, M. Häser, R. Ahlrichs, *Chem. Phys. Lett.* **1995**, *240*, 283–290.
- [144] K. Eichkorn, F. Weigend, O. Treutler, R. Ahlrichs, *Theor. Chem. Acc.* **1997**, *97*, 119–124.